

# Northumbria Research Link

Citation: Bristow, Charlie, Holmes, Jonathan, Matthey, Dave, Salzmann, Ulrich and Sloane, Hilary (2018) A late Holocene palaeoenvironmental 'snapshot' of the Angamma Delta, Lake Megachad at the end of the African Humid Period. *Quaternary Science Reviews*, 202. pp. 182-196. ISSN 0277-3791

Published by: Elsevier

URL: <https://doi.org/10.1016/j.quascirev.2018.04.025>  
<<https://doi.org/10.1016/j.quascirev.2018.04.025>>

This version was downloaded from Northumbria Research Link:  
<http://nrl.northumbria.ac.uk/id/eprint/34105/>

Northumbria University has developed Northumbria Research Link (NRL) to enable users to access the University's research output. Copyright © and moral rights for items on NRL are retained by the individual author(s) and/or other copyright owners. Single copies of full items can be reproduced, displayed or performed, and given to third parties in any format or medium for personal research or study, educational, or not-for-profit purposes without prior permission or charge, provided the authors, title and full bibliographic details are given, as well as a hyperlink and/or URL to the original metadata page. The content must not be changed in any way. Full items must not be sold commercially in any format or medium without formal permission of the copyright holder. The full policy is available online: <http://nrl.northumbria.ac.uk/policies.html>

This document may differ from the final, published version of the research and has been made available online in accordance with publisher policies. To read and/or cite from the published version of the research, please visit the publisher's website (a subscription may be required.)

**Accepted version**

Last updated 25-Apr-2018

**A late Holocene palaeoenvironmental ‘snapshot’ of the Angamma Delta, Lake  
Megachad at the end of the African Humid Period.**

Charlie S. Bristow<sup>1</sup>, Jonathan A. Holmes<sup>2</sup>, Dave Matthey<sup>3</sup>, Ulrich Salzmann<sup>4</sup>, Hilary J.  
Sloane<sup>5</sup>

1. Department of Earth and Planetary Sciences, Birkbeck University of London,  
Malet Street, London WC1E 7HX

2. Environmental Change Research Centre, Department of Geography, University  
College London, Gower Street, London, WC1E 6BT, UK

3. Department of Earth Sciences, Royal Holloway, University of London, Egham,  
Surrey, TW20 0EX, UK

4. Department of Geography and Environmental Sciences, Northumbria University,  
Ellison Place, Newcastle upon Tyne, NE1 8ST, UK

5. NERC Isotope Geosciences Facilities, British Geological Survey, Keyworth,  
Nottingham, NG12 5GG, UK

Keywords: Holocene; Palaeoecology; Sedimentology; Stable isotopes; Central  
Africa; Lake Megachad

**Abstract**

During the African Humid Period (AHP) there was a dramatic increase in the area of lakes and wetlands. Lake Megachad, one of several huge lakes, underwent dramatic fluctuations during the AHP prior to regression in the mid Holocene. However, the timing and nature of AHP termination has been disputed. We present evidence from sediments of the Angamma Delta, from the northern end of the palaeolake, for Lake Megachad lake-level fluctuations at the end of the AHP. Delta slope deposits were deposited over 7000 cal BP at the height of the AHP. Overlying bioclastic sediments, from 4300 – 4800 cal BP and an elevation of 285 – 290 m, lie below the palaeolake highstand (339 m) but close to the elevation of the Bahr el Ghazal sill, which divided the lake's two sub-basins. Ostracod  $\delta^{18}\text{O}$  values indicate that the waters of the northern sub-basin were evaporated to levels similar to modern Lake Chad. Palaeoecological evidence suggests that the lake was perennial and evaporative enrichment is attributed to restricted circulation of lake waters as the sill emerged. The age and elevation of the bioclastic sediment, coupled with published lake level reconstructions, suggests a complex lake-level history with a major regression at the end of the AHP, followed by a short lived, lake level rise after the followed by a transgression. This new evidence for changes in lake level provide support for other geological records and some modelling experiments that suggest rapid fluctuations in hydroclimate at the end of the AHP.

51

52 **1. Introduction**

53 From the late glacial until the mid Holocene, northern Africa was characterised by  
54 increases in effective moisture (precipitation minus evaporation, or  $P - E$ ) as a result  
55 of orbitally-forced strengthening of the African summer monsoon (Kutzbach and Liu,  
56 1997). During this interval, known as the African Humid Period (AHP – de Menocal  
57 et al., 2000), there was an increase in the extent of lakes and wetlands over large  
58 parts of northern Africa (Holmes and Hoelzmann, 2016), and shrubland and  
59 grassland replaced desert vegetation (Hoelzmann et al. 2004; Le 2017). The AHP  
60 was interrupted by millennial-scale arid intervals during the late glacial stadial and on  
61 several occasions during the Holocene; these intervals may have been accompanied  
62 by southward shifts in the intertropical convergence zone (ITCZ), in situ weakening of  
63 the summer monsoon and accompanying reduction in rainfall, and/or reductions in  
64 the latitudinal extent of the African rain-belt that were symmetrical over both  
65 hemispheres (Shanahan et al., 2015). The AHP came to an end in the mid Holocene  
66 sometime between around 6000 and 5000 BP, with palaeoenvironmental evidence  
67 and modelling experiments variously suggesting an abrupt, regionally-synchronous  
68 termination (e.g. de Menocal et al., 2000), a gradual ending (Kroepelin et al., 2008,  
69 Francus et al., 2013) or a pattern of progressive drying on which was superimposed  
70 increased short-term climatic variability (Gasse 2006, Renssen et al. 2006).

71 Understanding the nature and timing of AHP termination is important because it  
72 sheds light on the non-linear response of the African monsoon to orbital forcing and  
73 the role of vegetation and land-surface feedbacks (Claussen, 2009) and well as  
74 having implications for the human occupation of northern Africa during the Holocene  
75 (Manning and Timpson, 2014).

76

77 During the AHP, a huge palaeolake, known as Lake Megachad, occupied a large  
78 endorheic basin in the central part of North Africa. The basin extends from 6° to 25°  
79 north, spanning present-day subtropical to arid climatic zones. Water levels in the  
80 basin have fluctuated in response to the strength of the West African summer  
81 monsoon (Armitage et al., 2015). At its early to mid-Holocene peak, Lake Megachad  
82 was around 1000 km long (N-S) and up to 600 km wide (E-W); lake levels reached  
83 330 m (above present-day sea level), above which the lake spilled south into the  
84 Benue River (Drake and Bristow 2006). Lake Chad is now greatly reduced in extent,  
85 is currently around 200 km long and up to 150 km wide and covers roughly 5% of its  
86 former area. The lake surface lies at an elevation of 280 m, is confined to the  
87 southern half of the basin and supplied with around 90% of its waters through the  
88 Chari River. The northern half of the basin, the Bodélé Depression, is deeper with a  
89 low-point of 170m. This northern sub-basin is dry despite its greater depth, and is  
90 separated from Lake Chad by a 285-m-elevation sill that currently prevents water  
91 from flowing north from Lake Chad into the Bodélé Depression, although in the past,  
92 water has flowed in this direction through a river system known as the Bahr el  
93 Ghazal when the lake level exceeded 285 m. The changes in the extent and  
94 elevation of Lake Chad that occurred during the Holocene are amongst the most  
95 dramatic climatically driven changes on Earth.

96

97 During the AHP, the Sahara-Sahel boundary shifted in central and eastern Africa as  
98 far as 23°N (Hoelzmann et al., 2004). Tropical trees and shrubs occurred about 400-  
99 500 km north of their present distribution, mainly as part of the gallery-forest  
100 communities along the abundant rivers and lakes (Watrín et al, 2009). Most pollen

records from the Sahelian and Sudanian zone indicate a shift towards drier vegetation accompanied by a distinct decrease in lake levels between 6000 - 3000 cal BP. The two pollen records available for the Lake Chad Basin provide a rather inconsistent picture of the termination of the AHP. Whereas a record from the southern pool (Amaral et al. 2013) suggest a gradual retreat of trees and shrubs that indicated a humid climate from ca. 6050 cal BP onwards, the Tjeri sequence (Maley, 1981), further to the north-east, records a comparable change in vegetation composition approximately 2000 years later. The influence of anthropogenic activities on the West African landscape at the end of the AHP is a matter of debate. Archaeological evidence suggests that with the introduction of pastoralism and agriculture, ca. 4500 years ago, West Africa experienced a significant cultural and environmental transformation along with an increase in human population (McIntosh and McIntosh, 1983). However, to date, a large-scale human impact on the Sahelian and Sudanian savanna has not been detected in the geological records (e.g. Salzmann and Waller, 1998; Salzmann et al., 2002; Waller et al. 2007).

We investigated sediments from the Angamma Delta, in the northern part of the palaeolake, and from the Bodélé Depression, in order to provide constraints on lake-level changes at the end of the AHP, and to characterise the environment of the Bodélé Depression as it desiccated, using a combination of sedimentology, geochronology, micropalaeontology and isotope analysis. The sediments of the Falaise d'Angamma were interpreted to be a Holocene delta by Servant et al. (1969), who described volcanic breccias and tuffs at the base of the section overlain by layers of deltaic sediments that dip gently towards the South and Southwest. They describe a 20-30m series of rhythmic alternations of silts, clays and sands with a

range of sedimentary structures including cross-strata, slumps and channels. They also identified fossil wood, and bones of animals including an ancient form of Elephant *Loxodonta africana* and a small form of Hippopotamus as well as a cranio-facial fragment of a hominin, and conducted some radiocarbon dating of shells and carbonate concretions that provided an early Holocene age (Servant et al. 1969).

## 2. Materials and methods

The Angamma delta is located at the northern end of palaeolake Megachad (Fig. 1). The beach ridge along the top of the delta front stands at an elevation over 330m (Drake and Bristow 2006), and the delta slopes down to the basinal sediments that are composed of mudstones and diatomite at elevations below around 240m. The morphology of the delta is very well preserved and its deposits are locally very well exposed in a series of canyons incised into the western margin of the delta front (17° 36' 54" N, 17° 36' 11" E). A 25m sedimentary log was measured through the outcrop at a scale of 1:50 (Fig. 2). A sample of sand (CH36) was collected at 5m on the log, a sample of charcoal (CH37) was collected at 9m on the log, and bioclastic silty sands CH38 and CH39 were collected at 20 and 23m respectively. In addition, we have analysed a sample of the lakebed sediments from localities CH59 and CH60 (16° 48' 19.0" N 17° 48' 35.3" E and 16° 47' 17.6" N, 17° 50' 13.2" E, respectively), which lie at an elevation of 175m and close to the base of the Bodélé Depression.

Bulk sediment samples for faunal analysis were taken from CH38, CH39 and CH60. Dried bulk sediment was dispersed in tap water, sieved through a 250µm mesh and the coarse fraction dried in an oven at 105°C: ostracod and mollusc shells were extracted from this fraction under low-power stereo microscope and stored in

micropalaeontological slides (ostracods) or glass vials (mollusc shells). Quantitative counts of ostracods were undertaken whereas only the presence of individual mollusc taxa was noted. Selected ostracod specimens were measured (length and height) using a calibrated reticule under a low power (18.75x magnification) stereo microscope. Selected, well-preserved ostracod shells were brush-cleaned with methanol for oxygen and carbon isotope analysis: either single or multiple-shell samples were analysed depending on the species. Stable-isotope analyses on samples in the range 15 - 200ug were undertaken using an Isorime Multiprep and dual inlet mass spectrometer system at Royal Holloway, University of London (RHUL) and NIGL Keyworth, and the results reported in standard delta units relative to V-PDB. The external analytical reproducibility was better than  $\pm 0.07$  ‰ for both  $\delta^{18}\text{O}$  and  $\delta^{13}\text{C}$ .

Four sediment samples (CH38, CH39, CH59, CH60) were processed for pollen analysis using standard laboratory techniques (Faegri and Iversen, 1989), including HF treatment and acetolysis. *Lycopodium clavatum* spore tablets were added to each sample to allow calculation of pollen concentration (Stockmarr, 1971). Pollen and spores have been identified using the pollen reference collection held at Northumbria University.

Radiocarbon dating was undertaken on specimens of ostracods and molluscs, and on charcoal at the NERC Radiocarbon Laboratory and Beta Analytic. Radiocarbon dates were calibrated using IntCal13 (Reimer et al., 2013).

### 3. Results



### 3.1 Angamma Delta Geomorphology

The northern shoreline of palaeolake Mega-Chad is dominated by the Angamma delta which is around 50 km wide. Satellite images show remarkable preservation of the delta's geomorphology, including distributary channels on the delta top, beach ridges on the western side of the delta, a clearly defined beach ridge along the delta front, and cusate forelands to the east (Fig. 2a). The delta was fed by a braided fluvial distributary that flowed into the lake from the Tibesti Mountains in the north. These channels can be picked out on the satellite image cutting through some older beach ridges preserved on the delta top (Fig. 2b). However, the channels do not cut through the beach ridge which defines the delta front, which is known as the cordon littoral (Servant et al., 1969). The fact that the beach ridge is not cut by the fluvial distributary channels indicates that the fluvial drainage from the northern catchments ceased before the lake-level fell (Armitage et al. 2016). Had the rivers continued to flow after the lake-level had fallen, then the rivers would have incised through the beach ridge to create a falling stage delta. The planform of the delta front, which is defined by the cordon littoral, shows that the Angamma delta had a cusate morphology. Cusate deltas are characteristic of wave dominated deltas (Galloway 1975) indicating that sediment delivered to the delta front by rivers was reworked and redistributed by waves in the lake. The waves that impacted the northern shores of the palaeolake would have been driven by southwesterly monsoon winds (Drake and Bristow 2006) which had a maximum fetch of over 800 km from the southern shores of the lake. A topographic profile from the Angamma Delta to the Bodélé Depression preserves the lake bathymetry (Figure 2c). The cordon littoral stands at an elevation of around 339 m, which is 170 m above the lowest point in the Bodélé Depression, indicating that the lake was up to 170 m deep. Topographic profiles

across the delta front reveal a sigmoidal profile. The overall slope of the delta front is around 2° with the steepest part dipping at 10-12°. While most of the delta top morphology is well preserved there has been some erosion of the delta front and this is most obvious on the western side of the delta, which has been incised by steep sided gullies. These gullies, which do not cut the preserved shoreline, have steep headwalls with very small catchments and are interpreted to have formed by groundwater sapping after the lake level fell. Spring systems that might once have fed the gullies have long since dried up and the gullies and interfluvies have been eroded by the north-easterly Harmattan wind forming giant yardangs (Fig. 3a). The erosion provides excellent exposure of the Angamma Delta sediments, which are described and interpreted below.

### 3.2 Angamma Delta Sediments

The sediments of the Angamma Delta are very well exposed in a series of NE-SW trending canyons and cliff sections that are perpendicular to the delta front. The base of the Angamma delta sediments is underlain by volcanic breccias and tuffs (Servant et al. 1969). These are overlain by diatomite deposits with shells of *Pisidium* sp. and *Valvata* sp., which have been radiocarbon dated at  $9260 \pm 140$  <sup>14</sup>C yr BP and  $10160 \pm 160$  <sup>14</sup>C yr BP (Servant et al. 1969). A fine-grained carbonate concretion within the overlying sediments has a radiocarbon age of  $6050 \pm 150$  <sup>14</sup>C yr BP (Servant et al. 1969). The section described in this paper is on the western side of the delta where 25 m of Holocene sediments are exposed. This corresponds with the 20-30 m series of rhythmic alternations of silts, clays and sands described by Servant et al. (1969). The grainsize of the sediments, bed thickness and sedimentary structures are recorded on a graphic sedimentary log (Fig. 4). The sediments are composed of silts

and very-fine to fine-grained sands with a few thin layers of intraformational conglomerates (Fig. 4). Beds are generally thinner at the base of the section and thicker towards the top. Bed contacts are mostly sharp, many have erosional bases and a few fine up with gradational tops. Sedimentary structures include: current ripple lamination, wave ripple lamination, hummocky and swalley cross-stratification, bioturbation and soft sediment deformation (Fig. 4). Current ripple lamination is very common in the lower half of the section (Fig. 4) with a palaeocurrent direction of 250° which is attributed to currents flowing from the delta down-slope towards the lake bed. It is possible that some of these currents could be density driven turbidity currents. Some of the fine-grained sandstone beds (4-5 m on log, Fig. 4) have sharp erosive bases with intraformational mudstone clasts and fine upwards (Fig. 3b). They show many of the features of turbidite deposits including a sharp erosive base, fining upwards, and planar lamination and current ripple lamination (Bouma 1962). Turbidite deposits are common in lake sediments (e.g. Dyni and Hawkins 1981, Sturm and Matter 1978) and it is possible that dense, sediment-laden, flows from flood events on the rivers that supplied sediment to the delta continued to flow across the lake bed as turbidity currents, because the sediment-laden river water was denser than the freshwater within the lake. One palaeocurrent direction trending towards 250° is consistent with gravity driven flows down the southwest-facing delta slope. Wave driven current flows within palaeolake Mega-Chad have been modelled by Bouchette et al. (2010); their model suggests westward flowing surface currents and weak bottom currents driven by the north easterly Harmattan wind, and northeast flowing surface currents and weak bottom currents driven by the south-westerly monsoon wind around the Angamma delta.

An isolated set of wave ripple lamination is recorded close to the base of the section (1.3 m on the log, Fig. 4), a bed of wave ripple lamination is also recorded at 17 to 18 m on the log (Fig. 4). Wave ripple lamination indicates that the lake-bed is within wave-base and hence exposed to the oscillatory currents set up by surface wind-driven waves.

Hummocky cross-stratification is recorded at 5.5, 6, and 11 - 12, m on the log (Fig. 4), while swaley cross-stratification is recorded at 16.5 and 18m (Fig. 3c).

Hummocky Cross-stratification (HCS) is an indication of storm conditions most often associated with shallow marine environments (e.g. Duke 1985, Cheel and Leckie 1993), but has also be described in lacustrine sediments (Eyles and Clark 1986).

Wave tank experiments by Dumas and Arnott (2006) demonstrate that HCS can be developed under combined oscillatory and unidirectional currents, which are believed to occur in nature during storms when waves interact with unidirectional (offshore) currents. The preservation of HCS is aided by deposition of fine sand eroded from the upper shoreface during storm conditions. Dumas and Arnot (2006) suggest that swaley cross stratification can be formed under similar flow condition to HCS, but with lower rates of aggradation which preserve the swales rather than the hummocks. In their model swaley cross-stratification is found in slightly shallower water, closer to the shore than HCS, which is consistent with the observations that swaley cross-stratification occurs above the HCS in the Angamma delta log (Fig. 4). The possible wave ripple lamination on the top of one of the sharp-based fining-upwards beds at 4.5 m on the log (Fig. 4) suggests that these could be tempestites rather than turbidites.

Soft sediment deformation is very common and includes dewatering structures (3 m on log, Fig. 4), load structures (9.8 m on log), folded cross-strata (7.8 and 14 – 14.5 m on log) as well as extensional slides and injection structures. Servant et al (1969) also noted the presence of contorted beds from slumping in nearby sections. Overlying the interbedded sandstones and siltstones at the top of the measured section are brown, silty sands with abundant ostracods and gastropods. They are poorly indurated, and thus eroded more, and less well exposed than underlying beds.

### 3.3 Sandbody geometry

The canyons incised into the delta reveal a dip-section perpendicular to the delta front. The bedding geometry is lens-like, with a series of low-angle erosion surfaces cutting down to the west (Fig. 5). Some of the lenses are formed by channels because both channel banks can be observed in the field (Fig. 5). However, other erosion surfaces cut down from west to east and the opposite 'channel' bank is missing. The succession off-laps towards the west, into the lake. However, many of the beds are truncated by asymmetric and lens-like scour surfaces that cut down to the west (Fig. 5). Although the succession is broadly progradational there is an absence of obvious progrades and the origin the erosion surfaces is not certain, they might have been driven by changes in lake level, storm events or slumping. Similar looking, but slightly smaller scours within heterolithic distal lower shoreface sediments have been interpreted as formed by storm-generated currents coincident with riverine sediment influx 'storm floods' (Onyenanu et al. 2018). A similar scenario for coincident riverine flooding and storms during an enhanced monsoon might explain the scours on the Angamma delta front.

### 3.4 Chronology

Radiocarbon dates (Table1) indicate that the middle part of the Angamma delta sequence dates to around 7300 cal BP whereas the fossiliferous upper unit dates to around 4300 – 4800 cal BP. Previous radiocarbon dates from Servant et al. (1969) suggest that the base of the Angamma Delta sequence dates to the earliest part of the Holocene. The sediments from the residual pool in the Bodélé Depression, represented by CH59 and CH60, date to around 1000 cal BP Table 1: Armitage et al., 2015).

### 3.5 Palaeontology and geochemistry

Ostracods were present in three of the four samples investigated and most abundant in CH38, even allowing for the larger size of that sample (Table 2). The assemblage in CH38 is dominated by *H. giesbrechtii* and, with the exception of *S. aculeata*, which is represented by a single specimen, adults and juveniles are present (Fig. 6, for *S. bicornis*). The other samples are characterised by lower abundances and diversity (Table 2), although many *S. bicornis* specimens were removed from CH39 for dating prior to enumeration. No ostracods were found in CH59. Molluscs were also present in three out of the four samples investigated, although the lack of material in CH39 probably reflects the sample processing methods rather than genuine absence of molluscs. Sample CH38 is the most diverse; CHG59 contains two gastropod species and one bivalve (*Coelatura aegyptiaca*); CH60 is dominated by *Coelatura aegyptiaca* (Table 3).

Stable isotope values in the ostracod shells show large variability both within and between levels for oxygen and within levels for carbon (Fig. 7, Table 4). Maximum and minimum  $\delta^{18}\text{O}$  values are seen in CH38 (+0.03 ‰) and CH60 (+9.88 ‰), respectively; corresponding values for  $\delta^{13}\text{C}$  are -3.18 ‰ and +2.73 ‰ (both in CH38). Values in CH38 reveal some inter-species differences for isotope signatures (Fig. 7). For oxygen the 1.3 to 1.5 ‰  $^{18}\text{O}$ -enrichment in *Candona* compared with the other three species analysed is the most marked difference. For carbon, *Sclerocypris bicornis* appears  $^{13}\text{C}$ -deplete compared with *H. giesbrechtii*, *Cytheridella tepida* and *Candona* cf. *neglecta*, have  $\delta^{13}\text{C}$  values that broadly fall between these two species. There is no covariance amongst  $\delta^{18}\text{O}$  and  $\delta^{13}\text{C}$  values (Fig. 7), either for the individual species or for the dataset as a whole. The small number of trace-element determinations on shells of *L. inopinata* gave values of between 2.73 mmol/mol (CH60) and 6.36 mmol/mol (CH38) (Table 4).

All processed sample residues show a high organic matter content. Identifiable pollen and spores, however, are only preserved in sample CH60. As the other samples have been taken from outcrops, it is very likely that palynomorphs have been destroyed by post-sedimentary processes. Sample CH60 has a concentration of 21,778 pollen/g dry weight. Diversity is very low with *Typha* (53.3%) and *Cyperaceae* (34.9) being most abundant, followed by *Poaceae* (5.3%) and *Chenopodiaceae* (6.6). Green algae, such as *Pediastrum*, occur in high numbers.

#### 4. Discussion

We combine the stratigraphical and sedimentological information from the Angamma Delta section and the Bodélé Depression with palaeoecological and geochemical

data, in order to develop a palaeoenvironmental synthesis for the middle and late Holocene intervals that these sediments represent.

#### 4.1 Stratigraphy and sedimentology

Deposition of the fine-grained, heterolithic, sediments of the delta front during the early to middle Holocene AHP is consistent with stratigraphic models for lacustrine sedimentation where sediment supply and the input of water from rivers is intimately linked so that high lake levels are coincident within increased fluvial sediment input e.g. (Bohacs et al. 2000). Sharp-based fine-grained sandstone beds that fine upwards are interpreted as the deposits of turbidity currents formed when dense sediment-laden flood waters entered the lake from the rivers that flowed across the top of the Angamma Delta. Lacustrine turbidites have been linked to storm events within lake catchments (e.g. Osleger et al., 2009), and it is possible to speculate that these might be driven by annual monsoon rains, but equally they could be due to heavy rainfall and floods from convective thunderstorms. The scour surfaces observed within the heterolithic deltaic sediments might also be associated with storm-generated currents coincident with riverine sediment influx (Onyenanu et al. 2018). Additional work on lateral continuity of beds, and the geometry of erosive scour surfaces, as well as correlation along strike around the delta front would be needed to test the potential for seasonality. Such reconstructions are likely to be complicated by erosion on the delta front and switching of distributary channel across the delta top that will have created breaks in deposition and diachronous changes in facies. Another possible explanation is that the turbidites were seismically triggered (Moernaut et al. 2014, 2017), which would be consistent with



the possible seismic triggering of widespread soft-sediment deformation. One explanation for the slumping is gravitational instability on the gently inclined delta slope. However, soft sediment deformation can also be triggered by seismic shock and similar deposits in Pleistocene deltaic and lake sediments have been interpreted as seismogenic (e.g. Gilbert et al. 2005, Moretti and Ronchi 2011). Moretti and Ronchi (2011) rejected an internal, autokinetic, trigger because the deformed sediments are similar to other beds in the succession that lack evidence for liquefaction or fluidisation. On this basis, it is possible to argue for an allokinetic (external) trigger such as an earthquake but alternative allokinetic triggers related to lake level changes or storm events cannot be ruled out. The interbedded sandstones and mudstones that include possible turbidite and tempestite deposits along with slumps and channels are interpreted as a delta-slope facies. The overlying bioclastic-rich silty-sands are less well exposed and the depositional environment is not as easy to reconstruct from the sediments alone. In order to reconstruct their depositional environment, we consider evidence from the faunal assemblage, oxygen and carbonate isotopes below.

## 4.2 Ostracods

Published information on the ecology of ostracod taxa is used for the palaeoecological interpretation of the ostracod assemblages from the Angamma Delta and Bodélé Depression sediments.

### 4.2.1 Taxonomic and ecological notes on the ostracod taxa

*Limnocythere inopinata* (Baird, 1843) (Fig. 8)

This species is a widespread benthic taxon found in the littoral of large lakes and in small lakes and ponds (Geiger, 1990; Meisch, 2000; Rossi et al., 2010; Van der Meeren et al., 2010). In the Holarctic, the species is almost always parthenogenetic, although pockets of sexual populations are found geographically and stratigraphically (Griffiths and Horne, 1999): previously-reported African occurrences are parthenogenetic (Martens, 1990). Sexual populations are common in North America (Delorme, 1971) and China (Yin et al., 1999; Zhang et al., 2015). North American sexual populations are commonly referred to *L. sappaensis*, although many authors regard this as a junior synonym of *L. inopinata*, a view subscribed to here. *Limnocythere inopinata* is strongly euryhaline, although in saline lakes is restricted to waters with an alkalinity/Ca ratio >1 (Forester, 1983). The species is intolerant of low dissolved oxygen (Geiger, 1990) but can tolerate seasonal desiccation (Rossi et al., 2010; Van der Meeren et al., 2010). In the Angamma Delta samples, the species is moderately common, with both males and females present; it also occurs in CH60 from the Bodélé Depression, in which it is the most common species.

#### *Cytheridella* cf. *tepida* Victor, 1987 (Fig. 8)

The genus *Cytheridella* is most commonly found in North and South America (Park et al., 2002) but has also been reported from Africa (Klie, 1944; Rome and De Deckker, 1977; Victor, 1987; Karanovic, 2009). The Angamma Delta specimens show some resemblance to *Cytheridella tepida* Victor 1987, which is known from Nigeria, where it is associated with vegetation-rich, gently flowing streams and springs. It is moderately abundant in the Angamma Delta samples

*Darwinula stevensoni* Brady and Robertson, 1870) (Fig. 8)

This is a common, cosmopolitan species (Mesich, 2000) also reported from East and North Africa (Martens, 1984a) in a wide range of habitats. It is characteristic of freshwater, although can tolerate elevated salinity up to 30 gL<sup>-1</sup> (Gandolofi et al., 2001; Van Doninck et al., 2003) and is found in bicarbonate waters as well as those dominated by chloride and sulphate (Mezquita et al., 1999). It shows brood care and so cannot tolerate desiccation (Griffiths and Butlin, 1994). It is moderately abundant in the Angamma Delta samples and a single specimen was recovered from sample CH60 from the Bodélé Depression.

*Candona* cf. *neglecta* Sars, 1887 (Fig. 8)

Members of the genus *Candona* are not widely reported from Africa (Martens, 1984b) although *C. neglecta* has been recorded from North Africa (Martens, 1984b). Given the morphological variability within *C. neglecta* and the similarity of its shell to that of several other species (Meisch, 2000) it is possible that the specimens from the Angamma Delta belong to another species, although they are referred to *Candona* cf. *neglecta* here. *Candona neglecta sensu stricto* is a commonly freshwater ostracod that prefers colder water but can tolerate elevated temperature and brackish coastal and continental water (Meisch, 2000). It is moderately common in the Angamma Delta samples.

*Heterocypris giesbrechtii* (G. W. Müller, 1898) (Fig. 8)

This species has been found in Central and East Africa, in waters that are temporary or that fluctuate in volume and salinity (Martens, 1984b), and in permanent saline ( $\leq 9.4$  ‰) waterbodies on Aldabra (McKenzie, 1971). It was also abundant as part of

a low diversity ostracod assemblage in late Holocene lake sediments from NE Nigeria (Holmes et al., 1998) and the Faiyoum, in Egypt (Keatings et al., 2010). In the Angamma Delta samples, it is the most abundant ostracod taxon; it also occurs in CH60 from the Bodélé Depression.

*Sclerocypris* cf. *bicornis* (G. W. Müller, 1900) (Fig. 9)

The specimens show some similarity to both *S. bicornis* (G. W. Müller, 1900) and *S. excerta* Sars 1924. Compared to *S. excerta*, the specimens from the Angamma Delta are more quadrate and show a less prominent posterior point; moreover, this species has not been found from the Sahara or Sahel region (K. Martens, pers. comm. 2017). Compared to *S. bicornis*, the specimens from the Angamma Delta are also more subquadrate; moreover, the juveniles lack the lateral tubercles seen in this species, although both tuberculate and non-tuberculate forms of the species have been recorded (K. Martens, pers. comm. 2017). Furthermore, *S. bicornis* has been reported from West Africa (Gauthier, 1929, 1951) and Egypt (Keatings et al., 2010). On these bases, the Angamma Delta specimens are referred to *Sclerocypris* cf. *bicornis*.

Along with other members of the genus (Martens, 1986, 1988), *Sclerocypris bicornis* is most commonly found in small pools, which may be ephemeral, although it has also been found as a minor component of the deepwater fauna of Lake Turkana and in the Late Holocene sediments of lake Qarun in the Faiyum, Middle Egypt, probably in association with shallow ( $\geq 8$  m), saline, permanent water (Flower et al., 2006; Keatings et al., 2010). The species is quite common in the Angamma Delta samples.

*Sarscypridopsis aculeata* (Costa, 1847) (Fig. 8)

This species is typical of smaller waterbodies and can tolerate seasonal desiccation; it is common in slightly saline waters, with an optimum salinity range of 5 – 10 ‰ and preference for Na-Cl-type waters (Ganning, 1971; Meisch and Broodbakker, 1993). In the Angamma Delta samples the species is represented by a single specimen.

#### 4.2.2 Interpretation of the ostracod assemblages

Previous work on ostracods from past and present Lake Chad is sparse. Gauthier (1939) described living ostracods from several sites on Lake Chad. Zamar and Tukur (2015) described a small collection of ostracods from sediments of the Bama Ridge, a beach ridge that lies between 320 and 338 m.a.s.l. to the west of the present-day lake and marks a mid Holocene highstand; however, some or all of the material appears to have been misidentified. Within the Lake Chad Basin, but beyond the Holocene extent of the megalake, Holmes (1997) described a small collection of wetland ostracod species and Holmes et al. (1998) examined mid to late Holocene ostracod assemblages from inter-dunal lake sediments. Despite the dearth of previous studies on ostracods in the Lake Chad region, a reasonable amount of ecological information is available for the species encountered, as noted above.

The presence of adult and juvenile ostracod shells suggests that the assemblages are in situ and have not been subjected to significant post mortem reworking. The taxa present are all essentially freshwater species although those for which information is available are also able to tolerate elevated salinity. The occurrence of *L. inopinata* suggests that if the water were saline, it must have had an alkalinity/Ca ratio >1 (Forester, 1983). Although the species present are found in a range of

habitats, the association of several of the taxa, especially *S. bicornis*, *H. giesbrechtii* and *C. tepida*, with small, shallow and fluctuating waterbodies, is notable.

#### 4.3 Molluscs

Brown (1994) has summarised studies on the modern molluscs from Lake Chad, based on Lévêque (1967), Mandahl-barth (1968) and Brown (1974) and this can be used to interpret the fossil assemblages reported here. Van damme (1984) reports mollusc assemblages from exposures of sediments from the Falaise d'Angamma that are attributed to early or Middle Pleistocene sediments, but which are probably Holocene. Böttcher et al (1972) also report mollusc assemblages the Falaise d'Angamma, but of early Holocene age, around 10,000 – 9200 cal BP. In both instances, many of the species are similar to those encountered in our investigations.

The molluscs present in the Angamma samples reported here inhabit a wide range of aquatic habitats (Table 3). Half of the taxa are absent from, or not normally found in, water that desiccate seasonally and at least two of the taxa are able to tolerate elevated salinity. Overall, the mollusc assemblages suggest that the palaeo-waterbody was permanent.

#### 4.4 Pollen

The absence of pollen from all but sample CH60 means that inferences about past vegetation are restricted to the Bodélé Depression during the late Holocene interval. The pollen assemblage and frequent *Pediastrum* in sample CH60 indicates that the sediment was deposited in a shallow water body with fringing bulrush (*Typha*) and

sedges (Cyperaceae). Abundant Chenopodiaceae pollen point to the presence of an arid environment with halophytic vegetation. The low pollen taxa diversity might have partly been caused by the small basin size and catchment. However, the absence of any trees or shrubs in the pollen assemblage suggests that the lake was located in a desert environment.

## 4.5 Ostracod shell chemistry

### 4.5.1 Oxygen isotopes

We use the ostracod-shell oxygen-isotope data to estimate the oxygen-isotope values for the palaeo-lake waters. The oxygen-isotope ratio of aquatic carbonate is determined by the temperature and water isotope composition of the water from which the carbonate precipitated and the factors can be described quantitatively using empirical equations such as that of Kim and O'Neil, (1997). Such equations assume equilibrium precipitation, yet it is well known that ostracods form shells that show offsets from equilibrium that are positive, but which vary between taxa (von Grafenstein et al., 1999; Decrouy, 2012). Of the species analysed here, members of the subfamily Candoninae have the best constrained vital offset, which is  $+2.2 \pm 0.15$  ‰ (von Grafenstein et al., 1999). Although higher offsets for Candoninae have been reported (up to +3; Decrouy, 2012), a value of +2.2 is probably appropriate for this particular location based on the likely chemical composition of the palaeo-lake water. Offsets for the other taxa are less certain. A value of  $\sim +1$  ‰ has been suggested for *Heterocypris* (Perez et al., 2013), which accords with data in Burn et al., 2016, although higher (+1.7 ‰: Lawrence et al., 2008) and lower (+0.54 ‰: Schwalb et al., 2002) values have also been suggested, albeit with a small sample size in the former case and large uncertainties over calcification conditions in the latter. For the

purpose of the present study, we use a value of +1 ‰. For *Cytheridella* a value of +1 ‰ has been suggested by Meyer et al. (2017) and between 0.1 and 1‰ by Perez et al. (2013), although poorly constrained in both cases. There are no published estimates of vital offsets for *Sclerocypris*; comparison of  $\delta^{18}\text{O}$  values for this species and co-occurring *Candona cf neglecta* in CH38 suggests a value of 0.88 ‰: a similar approach for *Heterocypris* and *Cytheridella* yields values of +0.4 and +0.6, respectively, both of which are lower than the values quoted above. However, the use of co-occurring ostracods of different species to calculate a vital offset is problematical because it assumes that the individuals calcified under the exact same conditions of water temperature and water isotope composition, which may not be the case. For this reason, we prefer to use the values quoted from the literature and cited above for *Heterocypris* and *Cytheridella*: the value of +0.88 is used for *Sclerocypris* in the absence of better data, but with the caveat that it is highly uncertain.

The offset-corrected  $\delta^{18}\text{O}$  values are used to calculate  $\delta^{18}\text{O}_{\text{water}}$  values using Kim and O'Neil (1997). In the absence of temperature data for central Africa during the late Holocene, we assume present-day values taken from Faya-Largeau, Chad (minimum = January, 20°C, maximum = 34°C, June: IAEA/WMO, 2018). The results of this exercise (Fig. 10) show large variability, which is unsurprising given uncertainties in the calcification temperature and the large variation in  $\delta^{18}\text{O}$  values in ostracod specimens at each level. However, the reconstructions do suggest that the ambient lake water was moderately to strongly evaporated compared to estimated rainfall and rainfall-derived runoff for the present-day. Modern water isotope data for the greater Lake Chad region are summarized in Bouchez et al. (2016). The



weighted mean annual  $\delta^{18}\text{O}_{\text{ppt}}$  value for the nearest IAEA GNIP station at N'Djamena, Chad, is  $-3.8 \pm 1.7 \text{ ‰}$  (IAEA/WMO, 2018).  $\delta^{18}\text{O}$  values for fluvial inputs vary between  $-6$  and  $+3 \text{ ‰}$  for the Chari-Logone (weighted mean annual value =  $-3 \text{ ‰}$ ) and  $-4$  to  $+8 \text{ ‰}$  (no weighted mean annual value quoted) for the Komadugu Yobe (Bouchez et al., 2016). The most negative values are associated with the summer monsoon and the most positive values with dry-season evaporative enrichment.  $\delta^{18}\text{O}$  values in the modern lake vary spatially, with the lowest values ( $-1$  to  $+4 \text{ ‰}$ ) in the Southern Pool, intermediate values ( $+4$  to  $+7 \text{ ‰}$ ) in the Archipelagos and highest values ( $+6$  to  $+8 \text{ ‰}$ ) in the Northern Pool.

#### 4.5.2 Carbon isotopes

The carbonate-isotope ratio of aquatic carbonate is determined by the  $\delta^{13}\text{C}$  value of total dissolved inorganic carbon (TDIC), which in turn is controlled by equilibration between TDIC and atmospheric  $\text{CO}_2$ , the balance between aquatic productivity and decay and inputs of soil-derived carbon from the catchment. The  $\delta^{13}\text{C}$  values therefore provide information about sources and cycling of carbon within the lake.

Complete equilibration between TDIC and the atmosphere would yield a  $\delta^{13}\text{C}_{\text{TDIC}}$  value that is between  $8.5 \text{ ‰}$  (at  $20^\circ\text{C}$ ) and  $7 \text{ ‰}$  (at  $34^\circ\text{C}$ ) higher than atmospheric  $\text{CO}_2$ , (Mook et al, 1974), which had a  $\delta^{13}\text{C}$  value of about  $-6.5 \text{ ‰}$  in the late Holocene: Leuenberger et al., 1992). Complete equilibration tends to occur in waters with long residence times. Aquatic plants utilizing TDIC for photosynthesis will preferentially fix  $^{12}\text{C}$ , leaving the residual TDIC  $^{13}\text{C}$ -enriched, whereas decay or organic matter releases  $^{12}\text{C}$ -enriched carbon to the TDIC pool (Kelts and Talbot, 1990). Soil-derived carbon reflects catchment vegetation: in an area of

predominantly C4 plants, it will lie in the range -9 to -16 ‰ (Smith and Epstein, 1971).

Variation in the carbon-isotope signatures probably reflects the ecological preferences of the different ostracod species, because  $\delta^{13}\text{C}_{\text{TDIC}}$  values vary over small distances in lakes. *Heterocypris giesbrechtii*, which (based on better-studied congeners, such as *H. incongruens*: Rossi and Menozzi, 1990) is most likely to be a swimming species, will have a carbon-isotope signature that reflects open-water TDIC. Members of the genera *Candona*, *Cytheridella* and *Sclerocypris* are epibenthic, and thus their lower  $\delta^{13}\text{C}$  values (especially those for *Sclerocypris* and *Cytheridella*), most likely reflect TDIC  $\delta^{13}\text{C}$  values that are influenced by the mineralization of  $^{13}\text{C}$ -deplete organic matter, pointing to an organic-rich substrate.

There is lack of covariance amongst the ostracod  $\delta^{18}\text{O}$  and  $\delta^{13}\text{C}$  values. Although this is often taken to indicate the existence of a hydrologically open system (Talbot, 1990), there is often a lack covariance amongst  $\delta^{18}\text{O}$  and  $\delta^{13}\text{C}$  values specifically for biogenic carbonates, such as ostracods, even in closed systems (e.g. Holmes et al., 1997), probably owing to local habitat controls on the isotopic composition of the dissolved inorganic carbonate from which the biogenic carbonate precipitated (Talbot, 1990),

#### 4.5.3 Trace elements

In Kajemarum Oasis, NE Nigeria, Sr/Ca ratios in shells of *Limnocythere inopinata* have been used as a proxy for past salinity. Values for the Angamma Delta samples and for the Bodélé Depression sample are towards the low end of the range seen in

Kajamarum Oasis (<1 to >10 mmol/mol). However, although it is tempting use this information to suggest that the Angamma waters were of low salinity, it is not certain that the same Sr/Ca – salinity relationship observed for Kajamarum also prevailed for Angamma.

#### 4.6 Palaeoenvironmental synthesis

The interbedded sandstones and mudstones that characterise the lower part of the Angamma delta deposits appear to be part of an early to middle Holocene progradational delta-slope succession deposited during the AHP. The age of 7253-7416 cal BP ( $1\sigma$ ) is consistent with the radiocarbon ages for the base of the delta published by Servant et al. (1969). It is reasonable to suggest that rivers flowing from the north were active at that time and this is supported by the presence of lakes in the Tibesti, such as the Trou au Natron, during the early to middle Holocene (Kroepelin et al. 2016). However, river discharge must have ceased before 5600  $\pm$  300 BP because the river channels on the delta top are truncated by the beach ridge along the edge of the delta top (Armitage et al. 2015).

The bioclastic silty sands that overlie the interbedded delta-slope facies are around 3000 years younger (Table 1) and appear to postdate the end of the (AHP) between about 6000 and 5000 cal BP (de Menocal et al. 2000; McGee et al., 2013). The palaeoenvironmental interpretation of this facies has important implications for the lake-level history of Lake Megachad at the end of the AHP. The occurrence of a number of ostracod species that are desiccation tolerant coupled with an inferred water isotope composition that is consistent with evaporative enrichment (Fig. 10), could indicate that the sediments had been deposited in small, seasonally-

desiccated waterbodies that had been isolated following the regression of the mega lake. This interpretation, if correct, would suggest that the lake had undergone regression by this time to an altitude lower than 285 – 290 m, the height of samples CH38 and CH39. However, some of the molluscs found in these samples cannot tolerate desiccation (Table 3) and while some of the ostracods are desiccation resistant (Table 2), none is restricted to such environments and some are unable to tolerate desiccation. The oxygen-isotope values point to evaporative enrichment of the waterbody, although not to values that are any greater than in the modern lake. The elevation of the bioclastic sediments coincides with the elevation of the Bahr el Ghazal sill. We suggest that the Bahr el Ghazal sill would have restricted the circulation of waters between the southern and northern sub-basins. Given the geomorphological evidence that influent streams from the north had dried up prior to 5700 BP, and almost all of the water flowing into the palaeolake were derived from the south through the Chari delta, with restricted flow from south to north through the Bahr el Ghazal, it is proposed that the northern sub-basin became slightly evaporated with positive  $\delta^{18}\text{O}$  values similar to those of the northern sub-basin of Lake Chad today. On balance then, the sedimentological, stratigraphical, palaeoecological and isotopic evidence, when considered collectively, is best interpreted as representing deposition in the littoral zone of the megalake. Given the elevation CH 38 and CH 39 well below the 339m Angamma highstand shoreline, it is possible that they represent a regressive deposit, formed as the lake level fell.

According to the reconstruction of Armitage et al. (2015) the level of palaeolake Megachad was even lower between 4.7 and 3.2 ka. The evidence for the low lake-level comes from OSL ages of dune sands in the Erg du Jourab (Mauz and Felix

Henningsen 2005) of  $4700 \pm 200$  OSL BP,  $4700 \pm 300$  OSL BP,  $3900 \pm 400$  OSL BP,  $3400 \pm 200$  OSL BP,  $3100 \pm 200$  OSL BP and  $3100 \pm 200$ ; the two older ages are from elevations of 242 m and 266m respectively. Their ages overlap with the calibrated radiocarbon ages for the shells from the Angamma delta, while their elevations are around 20 to 45 m lower than the bioclastic silty sands on the Angamma delta, and both locations included layers of diatomite above the dune sands demonstrating that the dunes had been flooded by a lake transgression. The younger dune sand samples are from elevations between 278 and 289 m, which are within 5 to 10m of the elevation of the bioclastic silty sands and the scenario that best fits the observations is that the lake level fell abruptly after 5500 cal BP to an elevation beneath that of the dunes (less than 242m) causing them to be reactivated. Using the published OSL dates of  $5400 \pm 500$  BP at 333 m a.s.l. and  $4700 \pm 200$  BP at 224 m a.s.l. (Armitage et al., 2015) suggests a lake regression of  $\sim 16 \text{ cm yr}^{-1}$ , which is within the interannual range of lake-level variations for the recent past. The dune age of 4700 BP overlaps the calibrated radiocarbon age for the bioclastic silty sands and this can be reconciled if the dune ages are interpreted as dune stabilisation ages, caused by a lake level rise and transgression at 4700 cal BP. This scenario is common in endorheic basins in the Sahara (Bristow and Armitage, 2016) but contrasts with groundwater-fed lakes, such as the Ounianga, that persists to this day (Kroepelin et al., 2008).

During the later stages of the lake within the Bodélé depression, the palaeoecological remains point to the existence of a small and shallow waterbody, which the oxygen-isotope data confirm was evaporated. Pollen assemblages indicate that the lake was fringed with emergent macrophytes and set within an arid

catchment. Despite evaporative enrichment, there is no palaeoecological evidence that this waterbody was saline, however, and it is possible that the very final stages of the lake are not represented by the samples that were investigated.

## **5. Conclusions**

Stratigraphic, palaeoecological and isotopic evidence from the Angamma Delta confirms that there were complex lake-level and palaeohydrological changes in Lake Megachad at the end of the African Humid Period. The cusate geomorphology of the Angamma delta indicates that it was wave dominated. However, within the delta front sediments, wave ripples are relatively rare and a combination of storms and fluvial floods are interpreted to control sedimentation. Storm waves shaped the delta top forming a beach and interacted with unidirectional (offshore) currents and a supply of fine grained sand to generate HCS within on the delta front. The succession appears to shallow up with HCS being replaced by swalley cross-strata higher in the section, possibly associated with increased sediment supply and deposition during fluvial floods. Storm events and the presence of contorted and slumped beds could be an indication of neo-tectonic movements within the Chad Basin. However, there are many possible trigger mechanisms for liquefaction in the Angamma delta including sediment loading, unloading due to erosion or changes in lake level, or storm events, and it is not possible to determine the trigger mechanism without further work. Integrating the chronology of the deltaic sediments with other published ages for palaeolake Mega-Chad suggests that lake level was at its maximum elevation around 5700 cal BP. The level then fell sharply, to an elevation well below that of the sill between Lake Chad and the Bodélé depression allowing reactivation of dunes at elevations of 242 and 266m. The lake level then rose again

flooding across the sill between Lake Chad and the Bodélé depression, transgressing across the dunes around 4700 cal BP and depositing the bioclastic silty sands on the Angamma delta. The radiocarbon ages of shells suggest that the lake transgression lasted for around 500 years before the water level fell beneath the level of the sill. During this time the ostracods and molluscs suggest a littoral lake environment with moderate evaporation of shallow waters. The final stages of the lake in the Bodélé depression, around 1000 cal BP were marked by a shallow, evaporated waterbody fringed by emergent macrophytes. Our results suggest that Lake Megachad did not undergo a single regression during the mid Holocene, but rather experienced a series of abrupt fluctuations. These findings may be consistent with evidence for fluctuating climate and environment at the end of the AHP (Liu et al., 2007; Kroepelin et al., 2008; Amaral et al., 2013).

## Acknowledgements

We thank Richard Preece, Tom White and Jon Ablett for help and advice with mollusc identifications; Koen Martens, Dave Horne, Patrick De Deckker and Andy Cohen for discussions about the ostracod taxa and their ecology; Melanie Leng for facilitating some of the stable isotope analyses; Miles Irving for drafting most of the figures; two anonymous reviewers for their constructive comments. Radiocarbon dates were supported by the UK Natural Environment Research Council Radiocarbon Facility Allocation 1216.0407.

## References

Amaral, P. G. C., Vincens, A., Guiot, J., Buchet, G., Deschamps, P., Doumnang, J.-C., and Sylvestre, F. 2013. Palynological evidence for gradual vegetation and

- 749 climate changes during the African Humid Period termination at 13°N from a  
750 Mega-Lake Chad sedimentary sequence, *Climate of the Past*, 9, 223-241,  
751 Armitage, S. J., Bristow, C. S. and Drake, N. A. 2015. West African monsoon  
752 dynamics inferred from abrupt fluctuations of Lake Mega-Chad. *Proceedings of*  
753 *the National Academy of Sciences of the United States of America*, 112, 8543–  
754 8548.
- 755 Bohacs, K.M., Carroll, A.R., Neal, J.E., and Mankiewicz, P.J. 2000. Lake-basin type,  
756 source potential, and hydrocarbon character: an integrated sequence-  
757 stratigraphic-geochemical framework, in E.H. Gierlowski-Kordesch and K. R.  
758 Kelts, eds., *Lake basins through space and time: AAPG Studies in Geology*  
759 46, 3-34.
- 760 Böttcher, U., Ergenzinger, P. J., Jaekel, S.-H., and Kaiser, K. 1972. Quartäre  
761 Seebildungen und ihre Mollusken-Inhalten Im Tibesti-Gebirge und seinen  
762 Rahmenbereichen der zentralen Ostsahara. *Zeitschrift für*  
763 *Geomorphologie*, 16, 182-234
- 764 Bouchette, F., Schuster, M., Ghienne, J-F., Denamiel, C., Roquin, C., Moussa, A.,  
765 Marsaleix, P., Duringer, P., 2010. Hydrodynamics in Holocene Lake Mega-  
766 Chad. *Quaternary Research*, 73, 226-236.
- 767 Bouchez, C., Goncalves, J., Deschamps, P., Vallet-Coulomb, C., Hamelin, B.,  
768 Doumnang, J.C. and Sylvestre, F. 2016. Hydrological, chemical, and isotopic  
769 budgets of Lake Chad: a quantitative assessment of evaporation, transpiration  
770 and infiltration fluxes. *Hydrology and Earth System Sciences*, 20, 1599-1619.
- 771 Bouma, A. H. 1962, *Sedimentology of some flysch deposits: a graphic approach to*  
772 *facies interpretation*. Elsevier pp.168.



- 773 Bristow, C. and Armitage, S. 2016. Dune ages in the sand deserts of the southern  
774 Sahara and Sahel. *Quaternary International*, 410, 46-57
- 775 Brown D. S. 1974. A survey of the Mollusca of Lake Chad, Central Africa. Appendix  
776 A - Report on a collection of Planorbidae and Ancyridae from Lake  
777 Chad submitted by Mrs N F McMillan. *Revue de Zoologie Africaine*, 88, 329-  
778 342
- 779 Brown D. S. 1994. *Freshwater Snails of Africa and Their Medical Importance*, Taylor  
780 & Francis, London, pp. 609 (2<sup>nd</sup> ed)
- 781 Burn, M. J., Holmes, J. A., Kennedy, L. M., Bain, A., Marshall, J. D., and Perdikaris,  
782 S. 2016. A sediment-based reconstruction of Caribbean effective precipitation  
783 during the 'Little Ice Age' from Freshwater Pond, Barbuda. *The Holocene*, 26,  
784 1237-1247.
- 785 Cheel, R.J., and Leckie, D.A., 1993, Hummocky cross-stratification. In: Wright, V.P.,  
786 (ed.) *Sedimentology Review*. Blackwell Scientific Publications, pp. 103-122.
- 787 Claussen, M. 2009. Late Quaternary vegetation-climate feedbacks. *Climate of the*  
788 *Past*, 5, 203–216.
- 789 de Menocal, P., Ortiz, J., Guilderson, T., Adkins, J., Sarnthein, M., Baker, L.,  
790 Yarusinskya, M. 2000. Abrupt onset and termination of the African Humid  
791 Period: rapid climate responses to gradual insolation forcing. *Quaternary*  
792 *Science Reviews*, 19, 347–361.
- 793 Decrouy, L. 2012. Biological and environmental controls on isotopes in ostracod  
794 shells. In: Horne, D.J., Holmes, J.A., Rodriguez-Lazaro, J. and Viehberg, F.  
795 (eds.) *Ostracoda as Proxies for Quaternary Climate Change*. *Developments in*  
796 *Quaternary Science*, 17, 165–181.

- 797 Delorme, L.D. 1971. Freshwater ostracodes of Canada, Part 5. Families  
798 Limnocytheridae, Loxoconchidae. Canadian Journal of Zoology, 49, 43-64.
- 799 Drake, N. and Bristow, C. 2006. Shorelines in the Sahara: geomorphological  
800 evidence for an enhanced monsoon from palaeolake Megachad. The  
801 Holocene, 16, 901–911.
- 802 Duke, W.L. 1985, Hummocky cross-stratification, tropical hurricanes and intense  
803 winter storms. Sedimentology, 32, 167-194.
- 804 Dumas, S., and Arnott, R.W.C. 2006. Origin of hummocky and swaley cross-  
805 stratification – The controlling influence of unidirectional current strength and  
806 aggradation rate. Geology, 34, 1073-1076.
- 807 Dyni, J.R., and Hawkins, J.E. 1981. Lacustrine turbidites in the Green River  
808 Formation, northwestern Colorado. Geology, 9, 235-238.
- 809 Eyles, N. and Clark, .M., 1986. Significance of hummocky and swalley cross-  
810 stratification in late Pleistocene lacustrine sediments in the Ontario Basin,  
811 Canada. Geology, 14, .679-682.
- 812 Faegri, K. and Iversen, J. 1989. Textbook of Pollen Analysis, (revised by Faegri, K.,  
813 Kaland, P. E. and Krzywinski, K.), Wiley & Sons, Chichester.
- 814 Flower, R.J., Stickley, C., Rose, N.L., Peglar, S., Fathi, A.A. and Appleby, P.G. 2006.  
815 Environmental changes at the desert margin: An assessment of recent  
816 paleolimnological records in Lake Qarun, Middle Egypt. Journal of  
817 Paleolimnology, 35, 1-24.
- 818 Forester, R.M. 1983. Relationship of two lacustrine ostracode species to solute  
819 composition and salinity: implications for palaeohydrochemistry. Geology, 11,  
820 435-438.

- 821 Francus, P., von Suchodoletz, H., Dietze, M., Donner, R. V., Bouchard, F., Roy, A.-  
822 J., Fagot, M., Verschuren, D. and Kröpelin, S. 2013. Varved sediments of  
823 Lake Yoa (Ounianga Kebir, Chad) reveal progressive drying of the Sahara  
824 during the last 6100 years. *Sedimentology*, 60,, 911–934.
- 825 Galloway, W.E. 1975. Process framework for describing the morphologic and  
826 stratigraphic evolution of deltaic depositional systems. In: Broussard, M. L.  
827 (ed.) *Deltas, Models for exploration*. Houston Geological Society. pp.87-98.
- 828 Gandolfi, A., Todeschi, E.B.A., Van Doninck, K., Rossi, V. and Menozzi, P. 2001.  
829 Salinity tolerance of *Darwinula stevensoni* (Crustacea, Ostracoda). *Italian*  
830 *Journal of Zoology*, 68, 61-67.
- 831 Ganning, B. 1971. On the ecology of *Heterocypris salinus*, *H. incongruens* and  
832 *Cypridopsis aculeata* (Crustacea: Ostracoda) from Baltic brackish-water  
833 rockpools. *Marine Biology*, 8, 271-279.
- 834 Gasse, F, 2006. Climate and hydrological changes in tropical Africa during the past  
835 million years. *Comptes Rendus Palevol*, 5, 35–43.
- 836 Gauthier, H. 1929. Cladoceres et ostracodes du Sahara Central. *Bulletin de la*  
837 *Société d'Histoire Naturelle de l'Afrique du Nord*, 20, 143-162.
- 838 Gauthier, H. 1951. Contribution à l'étude de la faune des eaux douces au Sénégal  
839 (Entomostraces). 2. Ostracodes. Minerva, Algiers, 171pp.
- 840 Gauthier, H. 1939. Contribution à l'étude de la faune dulcaquicole de la region du  
841 Tchad et particulièrement des Brandiopodes et des Ostracodes. *Bulletin de*  
842 *l'Institut Français d'Afrique Noire*, 1, 110-244.
- 843 Geiger, W. 1990. The role of oxygen in the distribution and recovery of the  
844 *Cytherissa lacustris* population of Mondsee (Austria). In: Danielopol, D.L.,  
845 Carbonel, P., Colin, J.P. (eds.), *Cytherissa* (Ostracoda) - the Drosophila of

- 846 Paleolimnology. Bulletin de l'Institut de Géologie du Bassin d'Aquitaine 47/48,  
847 167–189.
- 848 Gilbert, L., Sanz de Galdeano, C., Alfaro, P., Scott, G. and Lopez Garrido, A.C.  
849 2005. Seismic induced slump in early Pleistocene deltaic deposits of the Baza  
850 Basin (SE Spain). *Sedimentary Geology*, 179, 279-294. Griffiths, H.I. and  
851 Butlin, R.K. 1994. *Darwinula stevensoni*: a review of the biology of a persistent  
852 parthenogen. In: Horne, D.J. and Martens, K. (eds.) *The Evolutionary Ecology*  
853 *of Reproductive Modes in Nonmarine Ostracoda*. University of Greenwich  
854 Press, London, pp. 27–36.
- 855 Griffiths, H.I. and Horne, D.J. 1999. Fossil distribution of reproductive modes in non-  
856 marine ostracods. In: Martens, K. (ed.) *Sex and Parthenogenesis: Evolutionary*  
857 *Ecology of Reproductive Modes in Non-marine Ostracoda*. Dr. W. Backhuys,  
858 Leiden, pp. 101–118.
- 859 Hoelzmann P., Gasse F., Dupont L.M., Salzmann U., Staubwasser M., Leuschner  
860 D.C., and Sirocko, F. 2004. Palaeoenvironmental changes in the arid and  
861 subarid belt (Sahara-Sahel-Arabian Peninsula) from 150 ka to present. In:  
862 Battarbee R.W., Gasse F. and Stickley C. E. (eds.) *Past Climate Variability*  
863 *through Europe and Africa*. Kluwer: pp. 219-256.
- 864 Holmes, J.A. 1997. Recent non-marine Ostracoda (Crustacea) from Yobe State,  
865 Northern Nigeria. *Journal of African Zoology*, 111, 137-146.
- 866 Holmes, J. A. and Hoelzmann, P. 2017. The late Pleistocene-Holocene African  
867 Humid Period as Evident in Lakes. *Oxford Research Encyclopedia of Climate*  
868 *Science*, DOI: 10.1093/acrefore/9780190228620.013.531.

- 869 Holmes, J.A., Fothergill, P.A., Street-Perrott, F.A. and Perrott, R.A. 1998. A high-  
870 resolution Holocene ostracod record from the Sahel zone of Northeastern  
871 Nigeria. *Journal of Paleolimnology*, 20, 369-380.
- 872 Holmes, J.A., Street-Perrott, F.A., Allen, M.J., Fothergill, P.A., Harkness, D.D.,  
873 Kroon, D. and Perrott, R.A. 1997. Holocene palaeolimnology of Kajemarum  
874 Oasis, Northern Nigeria: An isotopic study of ostracodes, bulk carbonate and  
875 organic carbon. *Journal of the Geological Society*, 154, 311-319.
- 876 IAEA/WMO. 2018. Global Network of Isotopes in Precipitation. The GNIP Database.  
877 Accessible at: <http://www.iaea.org/water>.
- 878 Ibrahim, A. M., Bishai, H. M. and Khalil, M. T. 1999. Freshwater molluscs of Egypt.  
879 Publication of National Biodiversity Unit, No. 10.
- 880 Karanovic, I. 2009. Four new species of *Gomphodella* De Deckker, with a  
881 phylogenetic analysis and a key to the living representatives of the subfamily  
882 Timiriaseviinae. *Crustaceana*, 82, 1133–1176.
- 883 Keatings, K., Holmes, J., Flower, R., Horne, D., Whittaker, J.E. and Abu-Zied, R.H.,  
884 2010. Ostracods and the Holocene palaeolimnology of Lake Qarun, with  
885 special reference to past human-environment interactions in the Faiyum  
886 (Egypt). *Hydrobiologia*, 654, 155-176.
- 887 Kelts, K. and Talbot, M. 1990. Lacustrine carbonates as geochemical archives of  
888 environmental change and biotic/abiotic interactions. In: Tilzer, M.M. and  
889 Serruya, C. (eds.) *Large Lakes: Ecology, Structure and Function*, pp. 288-315.
- 890 Kim, S.T. and O'Neil, J.R., 1997. Equilibrium and nonequilibrium oxygen isotope  
891 effects in synthetic carbonates. *Geochimica et Cosmochimica Acta*, 61, 3461-  
892 3475.

- 893 Klie, W., 1944. Exploration du Parc National Albert. 12. Ostracoda. Institut des Parcs  
894 Nationaux du Congo Belge 12, 1-62.
- 895 Kroepelin, S., Verschuren, D., Lézine, A.M., Eggermont, H., Cocquyt, C., Francus,  
896 P., Cazet, J.P., Fagot, M., Rumes, B., Russell, J.M., Darius, F., Conley, D.J.,  
897 Schuster, M., von Suchodoletz, H. and Engstrom, D.R., 2008. Climate-driven  
898 ecosystem succession in the Sahara: The past 6000 years. *Science*, 320, 765-  
899 768.
- 900 Kroepelin, S., Dinies, M., Sylvestre, F., and Holzmann, P, 2016, Crater palaeolakes  
901 in the Tibesti Mountains (Central Sahara, north Chad), new insights into past  
902 Sahara climates. *Geophysical Research Abstracts*, 18, EGU2016 6557,  
903 CL1.16.
- 904 Kutzbach, J. E. and Liu, Z. 1997. Response of the African monsoon to orbital forcing  
905 and ocean feedbacks in the middle Holocene. *Science*, 278, 440–443.
- 906 Lawrence, J.R., Hyeong, K., Maddocks, R.F. and Lee, K.S. 2008. Passage of  
907 Tropical Storm Allison (2001) over southeast Texas recorded in  $\delta^{18}\text{O}$  values of  
908 Ostracoda. *Quaternary Research*, 70, 339-342.
- 909 Leuenberger, M., Siegenthaler, U. and Langway, C.C., 1992. Carbon isotope  
910 Composition of atmospheric  $\text{CO}_2$  during the Last Ice-Age from an Antarctic ice  
911 core. *Nature*, 357, 488-490.
- 912 Lévêque, C. 1967. Mollusques aquatiques de la zone est du Lac Tchad. *Bulletin de*  
913 *l'Institut Français d'Afrique Noire*, 29, 1494-1533
- 914 Lézine, A.M., 2017. Vegetation at the Time of the African Humid Period. *Oxford*  
915 *Research Encyclopedia of Climate Science*, DOI:  
916 10.1093/acrefore/9780190228620.013.530.

- 917 Liu, Z., Wang, Y., Gallimore, R., Gasse, F., Johnson, T., deMenocal, P., Adkins, J.,  
918 Notaro, M., Prenticer, I.C., Kutzbach, J., Jacob, R., Behling, P., Wang, L. and  
919 Ong, E. 2007. Simulating the transient evolution and abrupt change of  
920 Northern Africa atmosphereocean-terrestrial ecosystem in the Holocene.  
921 Quaternary Science Reviews, 26, 1818–1837.
- 922 Maley, J., 1981, Études palynologiques dans le bassin du Tchad et  
923 paléoclimatologie de l'Afrique nord-tropicale de 30.000 ans à l'époque actuelle.  
924 Thèse Sc., Montpellier, Travaux et Documents ORSTOM, Paris, 129 , 586 pp.
- 925 Mandahl-Barth, G. 1968. Mollusques d'eau douce. In: Symoens, J.J. (ed.)  
926 Exploration Hydrobiologique du bassin du Lac Bangweolo et  
927 du Luapula. Cercle Hydrobiol. 12, Cercle Hydrobiologique de Bruxelles, pp. 1-  
928 68.
- 929 Manning, K. and Timpson, A. 2014 The demographic response to Holocene climate  
930 change in the Sahara. Quaternary Science Reviews, 101, 28–35.
- 931 Martens, K. 1986; Taxonomic revision of the subfamily Megalocypridinae Rome,  
932 1965 (Crustacea, Ostracoda). Verhandelingen van de koninklijke Akademie  
933 voor Wetenschappen, Letteren en Schone Kunsten van België, Klasse der  
934 Wetenschappen, 48, 1-81.
- 935 Martens, K. 1984a. On the freshwater ostracods (Crustacea, Ostracoda) of the  
936 Sudan, with special reference to the Red Sea Hills, including a description of a  
937 new species. Hydrobiologia, 110, 137-161.
- 938 Martens, K. 1984b. Annotated checklist of non-marine ostracods Crustacea,  
939 Ostracoda, from African inland waters. Musée Royal de l'Afrique Centrale  
940 Tervuren - Belgique, Documentation Zoologique, 20, pp. 1-51.

- 941 Martens, K. 1988. Seven new species and two new subsepcies of  
942 *Sclerocypris* SARS, 1924 from Africa, with new records of some other  
943 Megalocypridinids (Crustacea, Ostracoda). *Hydrobiologia*, 162, 243-273.
- 944 Martens, K. 1990. Revision of African *Limnocythere* s.s. Brady, 1867 (Crustacea,  
945 Ostracoda), with special reference to the Rift Valley Lakes: morphology,  
946 taxonomy, evolution and (palaeo-) ecology. *Archiv Für Hydrobiologie*  
947 Supplement, 83, 453-524.
- 948 Mauz, B., and Felix-Henningsen, P. 2005. Palaeosols in Saharan and Sahelian  
949 dunes of Chad: Archives of Holocene North African climate change. *The*  
950 *Holocene*, 15, 453–458.
- 951 McGee, D., deMenocal, P.B., Winckler, G., Stuut, J.B.W. and Bradtmiller, L.I. 2013.  
952 The magnitude, timing and abruptness of changes in North African dust  
953 deposition over the last 20,000 yr. *Earth and Planetary Science Letters*, 371,  
954 163-176.
- 955 McIntosh S. K. and McIntosh R.J. 1983. Current directions in West African  
956 prehistory, *Annual Review of Anthropology*, 12, 215-258
- 957 McKenzie, K.G. 1971. Entomostraca of Aldabra, with special reference to the genus  
958 *Heterocypris* (crustacea, ostracoda). *Philosophical Transactions of the Royal*  
959 *Society, Series B* 260, 257-297.
- 960 Meisch, C. 2000. Freshwater Ostracoda of western and central Europe.  
961 *Süßwasserfauna von Mitteleuropa* 8/3. Gustav Fischer, Stuttgart.
- 962 Meisch, C. and Broodbakker, B. 1993. Freshwater Ostracoda (Crustacea) collected  
963 by Prof. J.H. Stock on the Canary and Cape Verde islands. With an annotated  
964 checklist of the freshwater Ostracoda of the Azores, Madeira, the Canary, the



- 965           Selvagens and Cape Verde islands, Ostracoda. Travaux Scientifiques du  
966           Musee National d'Histoire Naturelle de Luxembourg, Luxembourg, 3-47.
- 967 Meyer, J., Wrozyzna, C., Leis, A., Piller, W. 2017. Modeling calcification periods of  
968           *Cytheridella ilosvayi* from Florida based on isotopic signatures and  
969           hydrological data. Biogeosciences, 14, 4927-4947.
- 970 Mezquita, F., Tapia, G. and Roca, J.R. 1999. Ostracoda from springs on the eastern  
971           Iberian Peninsula: ecology, biogeography and alaeolimnological implications.  
972           Palaeogeography. Palaeoclimatology, Palaeoecology, 148, 65–85.
- 973 Moernaut, J., Van Dael, M., Heirman, K., Fontijn, K., Strasser, M., Pino, M., Urrutia,  
974           R. and DeBatist, M. 2014. Lacustrine turbidites as a tool for quantitative  
975           earthquake reconstruction: New evidence for variable rupture mode in south  
976           central Chile. Journal of Geophysical Research Solid Earth, 119, 1607-1633.
- 977 Moernaut, J., Van Dael, M., Strasser, M., Clare, M.A., Heirman, K., Viel, M.,  
978           Cardenas, J., Kilian, R., Ladron de Guevara, B., Pino, M., Urrutia, R. and  
979           DeBatist, M. 2017. Lacustrine turbidites produced by surficial slope sediment  
980           remobilization: A mechanism for continuous and sensitive turbidite  
981           paleoseismic records. Marine Geology, 384, 159-176.
- 982 Mook, W.G., Bommerson, J.C., and Staverman, W.H. 1974. Carbon isotope  
983           fractionation between dissolved bicarbonate and gaseous carbon dioxide.  
984           Earth and Planetary Science Letters, 22, 169-176.
- 985 Moretti, M., and Ronchi, A. 2011, Liquifaction features interpreted as seismites in the  
986           Pleistocene fluvio-lacustrine deposits of the Neuquen Basin (Northern  
987           Patagonia). Sedimentary Geology, 235, 200-209.
- 988 Onyenanu, G.I., Jacquemyn, C.E.M.M., Graham, G.H., Hampson, G.J., Fitch, P.J.R.,  
989           and Jackson, M.D. 2018. Geometry, distribution and fill of erosional scours in a

- 990 heterolithic, distal lower shoreface sandstone reservoir analogue: Grassy  
991 Member, Blackhawk Formation, Book Cliffs, Utah, USA. *Sedimentology*, 65,  
992 doi: 10.1111/sed.12444
- 993 Osleger, D.A., Heyvaert, A.C., Stoner, J.S., and Veroslub, K.L. 2009, Lacustrine  
994 turbidites as indicators of Holocene storminess and climate: Lake Tahoe,  
995 California and Nevada. *Journal of Palaeolimnology*, 42, 103-122.
- 996 Park, L. E., Martens, K. and Cohen, A. S. 2002. Phylogenetic relationships  
997 of *Gomphocythere* (Crustacea, Ostracoda) in Lake Tanganyika, East Africa.  
998 *Journal of Crustacean Biology*, 22, 15–27,
- 999 Perez, L., Curtis, J., Brenner, M., Hodell, D., Escobar, J., Lozano, S. and Schwalb,  
1000 A. 2013. Stable isotope values ( $\delta^{18}\text{O}$  and  $\delta^{13}\text{C}$ ) of multiple ostracode species in  
1001 a large Neotropical lake as indicators of past changes in hydrology.  
1002 *Quaternary Science Reviews*, 66, 96-111.
- 1003 Reimer, P. J., Bard, E., Bayliss, J. W., Beck, P. G., Blackwell, C. B., Ramsey, C. E.  
1004 Buck, H. Cheng, R. L. Edwards, M. Friedrich, P. M. Grootes, T. P. Guilderson,  
1005 H. Haflidason, I. Hajdas, C. Hatte, T. J. Heaton, D. L. Hoffmann, A. G. Hogg,  
1006 K. A. Hughen, K. F. Kaiser, B. Kromer, S. W. Manning, M. Niu, R. W. Reimer,  
1007 D. A. Richards, E. M. Scott, J. R. Southon, R. A. Staff, C. S. M. Turney, and J.  
1008 van der Plicht (2013), Intcal13 and Marine13 radiocarbon age calibration  
1009 curves 0-50,000 Years Cal BP, *Radiocarbon*, 55, 1869-1887.
- 1010 Renssen, H., Brovkin, V., Fichefet, T. and Goosse, H. 2006. Simulation of the  
1011 Holocene climate evolution in Northern Africa: The termination of the African  
1012 Humid Period. *Quaternary International*, 150, 95-102.
- 1013 Rome, D. R. and De Deckker, P. 1977. Ostracodes du Lac Kivu. *Mémoires de*  
1014 *l'Institut Géologique de l'Université de Louvain*, 29, 241–287.

- 1015 Rossi, V. and Menozzi, P. 1990. The clonal ecology of *Heterocypris incongruens*  
1016 (Ostracoda). *Oikos* 57, 388-398.
- 1017 Rossi, V., Piotti, A., Geiger, W., Benassi, G. and Menozzi, P. 2010. Genetic structure  
1018 of Austrian and Italian populations of *Limnocythere inopinata* (Crustacea,  
1019 Ostracoda): a potential case of post- glacial parthenogenetic invader? *Annales*  
1020 *Zoologici Fennici*, 47, 133–143.
- 1021 Salzmann, U. and Waller, M. 1998. The Holocene vegetational history of the  
1022 Nigerian Sahel based on multiple profiles. *Review of Palaeobotany and*  
1023 *Palynology*, 100, 39-72.
- 1024 Salzmann, U., Hoelzmann, P. and Morczineck, I. 2002. Late Quaternary Climate and  
1025 Vegetation of the Sudanian zone of NE-Nigeria. *Quaternary Research*, 58, 73-  
1026 83.
- 1027 Schwalb, A., Burns, S.J., Cusminsky, G., Kelts, K. and Markgraf, V. 2002.  
1028 Assemblage diversity and isotopic signals of modern ostracodes and host  
1029 waters from Patagonia, Argentina. *Palaeogeography. Palaeoclimatology,*  
1030 *Palaeoecology*, 187, 323-339.
- 1031 Servant, M., Ergenzinger, P. and Coppens, Y. 1969, Datations absolues sur un delta  
1032 lacustre quaternaire au Sud du Tibesti (Angamma). *Compte Rendu Sommaire*  
1033 *des Séances de la Société Géologique de France*. 8, 313-314.
- 1034 Shanahan, T. M., McKay, N. P., Hughen, K. A., Overpeck, J. T., Otto-Bliesner, B.,  
1035 Heil, C. W., King, K., Scholz, C. A. and Peck, J. 2015. The time-transgressive  
1036 termination of the African Humid Period. *Nature Geoscience*, 8, 140–144.
- 1037 Smith, B.N. and Epstein, S. 1971. Two categories of  $^{13}\text{C}/^{12}\text{C}$  ratios for higher plants.  
1038 *Plant Physiology*, 47, 380-384.

- 1039 Stockmarr, J. 1971. Tablets with spores used in absolute pollen analysis, Pollen et  
1040 spores, 13, 615–621.
- 1041 Sturm, M. and Matter, A. 1978, Turbidites and varves in Lake Brienz (Switzerland)  
1042 deposition of clastic detritus by density currents. In: Matter, A., and Tucker,  
1043 M.E., (eds.) Modern and Ancient Lake Sediments. International Association of  
1044 Sedimentologists, pp.147-168.
- 1045 Talbot, M.R. 1990. A review of the palaeohydrological interpretation of carbon and  
1046 oxygen isotope ratios in primary lacustrine carbonates. Chemical Geology  
1047 (Isotope Geosciences Section) 80, 261-279.
- 1048 Van damme, D. 1984. The freshwater Mollusca of Northern Africa. Developments in  
1049 Hydrobiology, 25, 1-164.
- 1050 Van der Meeren, T., Almendinger, J.E., Ito, E. and Martens, K. 2010. The ecology of  
1051 ostracodes (Ostracoda, Crustacea) in western Mongolia. Hydrobiologia, 641,  
1052 253-273.
- 1053 Van Doninck, K., Schon, I., Martens, K. and Goddeeris, B. 2003. The life-cycle of the  
1054 asexual ostracod *Darwinula stevensoni* (Brady & Robertson, 1870)  
1055 (Crustacea, Ostracoda) in a temperate pond. Hydrobiologia, 500, 331-340.
- 1056 Victor, R. 1987. A new species of the genus *Cytheridella* (Crustacea, Ostracoda)  
1057 from Nigeria, West Africa. Journal of Natural History, 21, 893-902.
- 1058 von Grafenstein, U., Erlernkeuser, H. and Trimborn, P. 1999. Oxygen and carbon  
1059 isotopes in modern fresh-water ostracod valves: assessing vital offsets and  
1060 autecological effects of interest for palaeoclimate studies. Palaeogeography.  
1061 Palaeoclimatology, Palaeoecology, 148, 133-152.

- 1062 Waller, Martyn P., Street-Perrott, F. A. and Wang, H. 2007. Holocene vegetation  
1063 history of the Sahel: pollen, sedimentological and geochemical data from  
1064 Jikariya Lake, north-eastern Nigeria. *Journal of Biogeography*, 34. 1575-1590.
- 1065 Watrin, J., Lézine, A.-M., Hely, C. and Contributors. 2009. Plant migration and plant  
1066 communities at the time of the "green Sahara". *Comptes Rendus Geoscience*  
1067 341, 656-670.
- 1068 Yin, Y. & Geiger, W. and Martens, K. 1999. Effects of genotype and environment on  
1069 phenotypic variability in *Limnocythere inopinata* (Crustacea: Ostracoda).  
1070 *Hydrobiologia*, 400, 85-114.
- 1071 Zarma A.A. and Tukur A. 2015. Stratigraphic Status of the Bama Beach Ridge and  
1072 the Chad Formation in the Bornu Sub-Basin, Nigeria. *Journal of Geoogy and*  
1073 *Geoscience*, 4,192. doi:10.4172/2329-6755.1000192.
- 1074 Zhang, W., Mischke, S., Zhang, C., Zhang, H. and Wang, P. 2015. Sub-Recent  
1075 Sexual Populations of *Limnocythere inopinata* Recorded for the First Time  
1076 from > 3500 m Altitude on the Tibetan Plateau. *Acta Geologica Sinica*,  
1077 89, 1041–1042.
- 1078  
1079  
1080  
1081  
1082  
1083  
1084  
1085  
1086  
1087

**Figures**

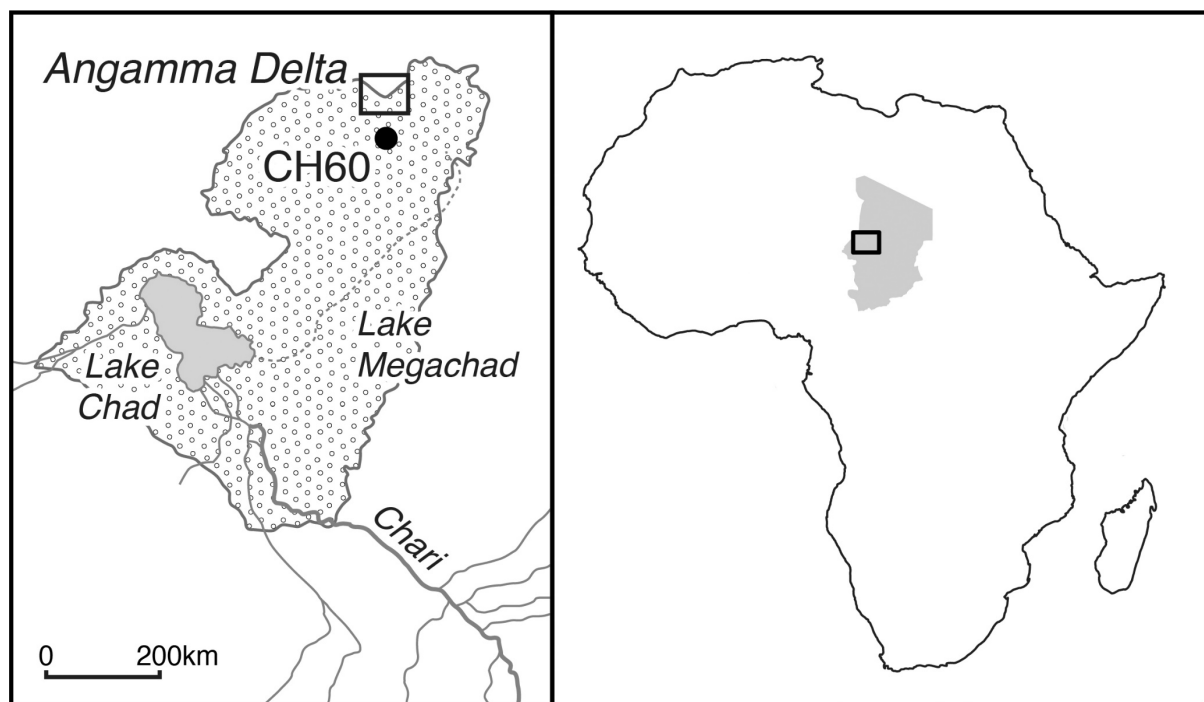


Fig. 1. Map of palaeolake Mega-Chad showing the location of the Angamma Delta at the northern end of the lake with a map of Africa inset.

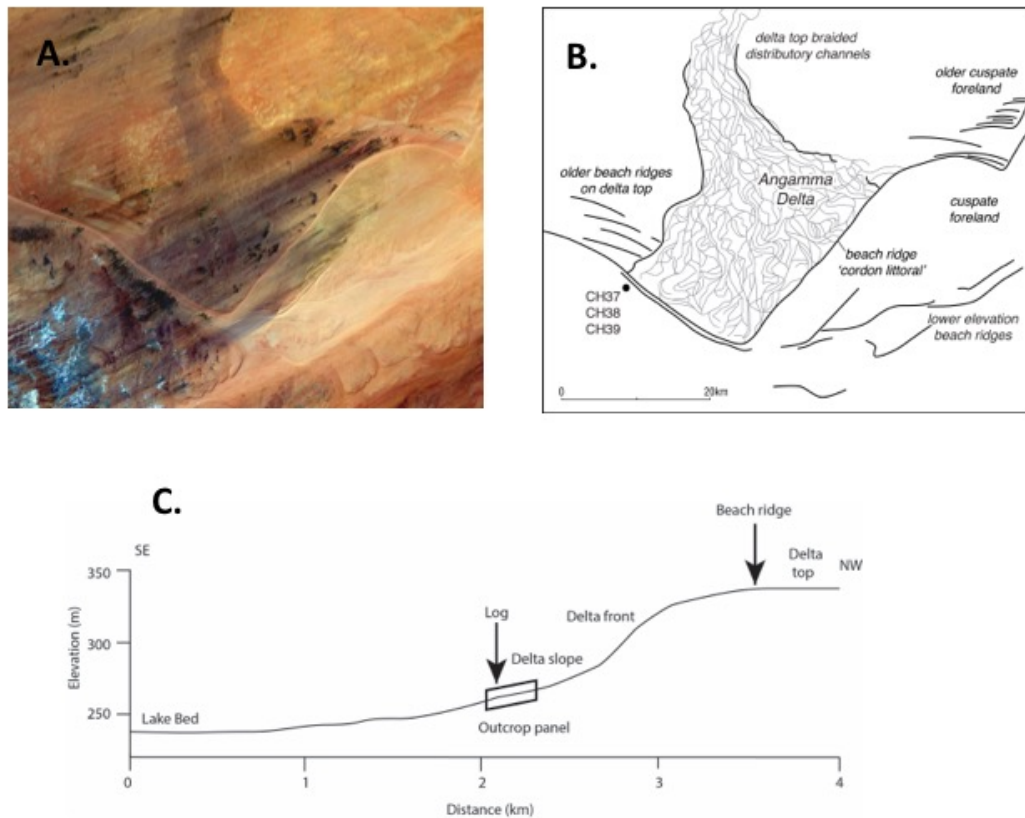
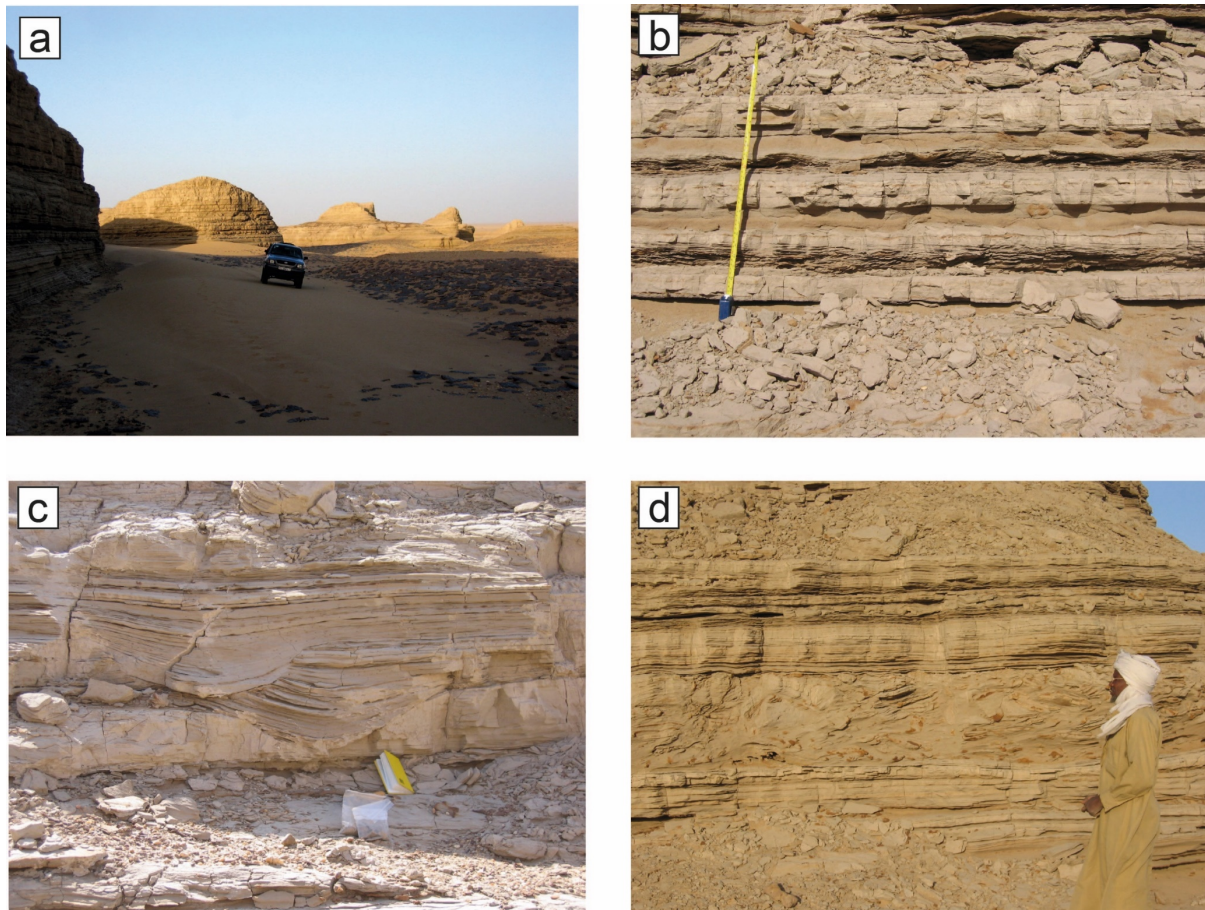


Fig. 2. A) Satellite image of the Angamma Delta. B) Geomorphological interpretation of the satellite image above showing beach ridges and the braided fluvial channels that are preserved on the delta top, modified from Drake and Bristow (2006) and

1117 Schuster et al. (2005). C) Topographic profile across the Angamma delta and the  
1118 northern part of the Bodélé depression that represents the palaeobathymetry of the  
1119 northern margin of the lake. Inset box shows the location of the sedimentary log and  
1120 the outcrop photograph.

1121



1122

1123 Fig. 3. Geomorphology and sedimentary structures and bedding within the  
1124 Angamma Delta.

1125 (a) Field photograph of giant yardangs eroded from the western margin of the  
1126 Angamma Delta, pick-up truck for scale.

1127 (b) Horizontal laminated siltstones interbedded with sharp based current ripple  
1128 laminated sandstones that are possible turbidite deposits, tape measure with  
1129 0.6 m rule for scale.



- 1130 (c) Swaley cross-strata interpreted to be formed during storm events, 19 cm field  
1131 note book for scale.
- 1132 (d) Partially fluidised bed with slump folds, disrupted and contorted bedding  
1133 underlain by horizontal sandstone beds and overlain by horizontal sandstone  
1134 beds, person for scale.



1139

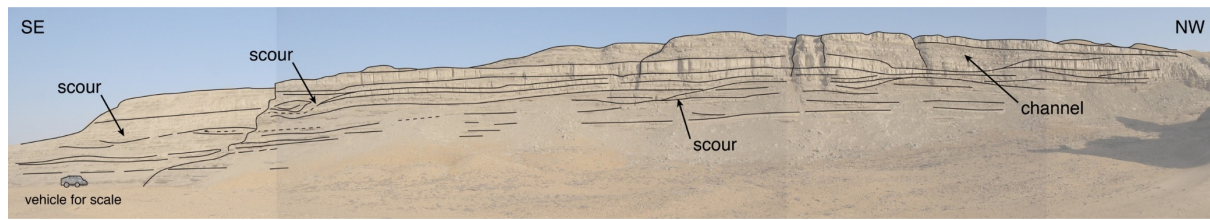
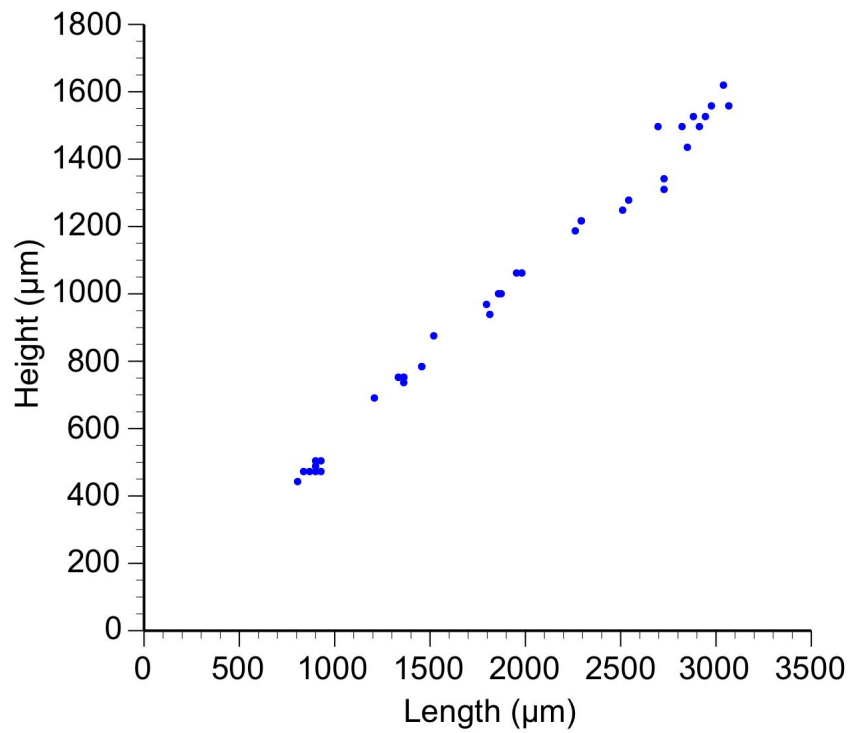


Fig. 5. Annotated photograph of canyon wall trending southeast - northwest and incised into the delta slope showing the geometry of the deltaic deposits that are cut by erosion surfaces defining lense-like sandbody geometries from channels (one of which is marked). Vehicle for scale lower left.



1155

1156

1157 Fig. 6. Length-height plot for specimens of *Sclerocypris* cf. *bicornis* from CH38

1158

1159

1160

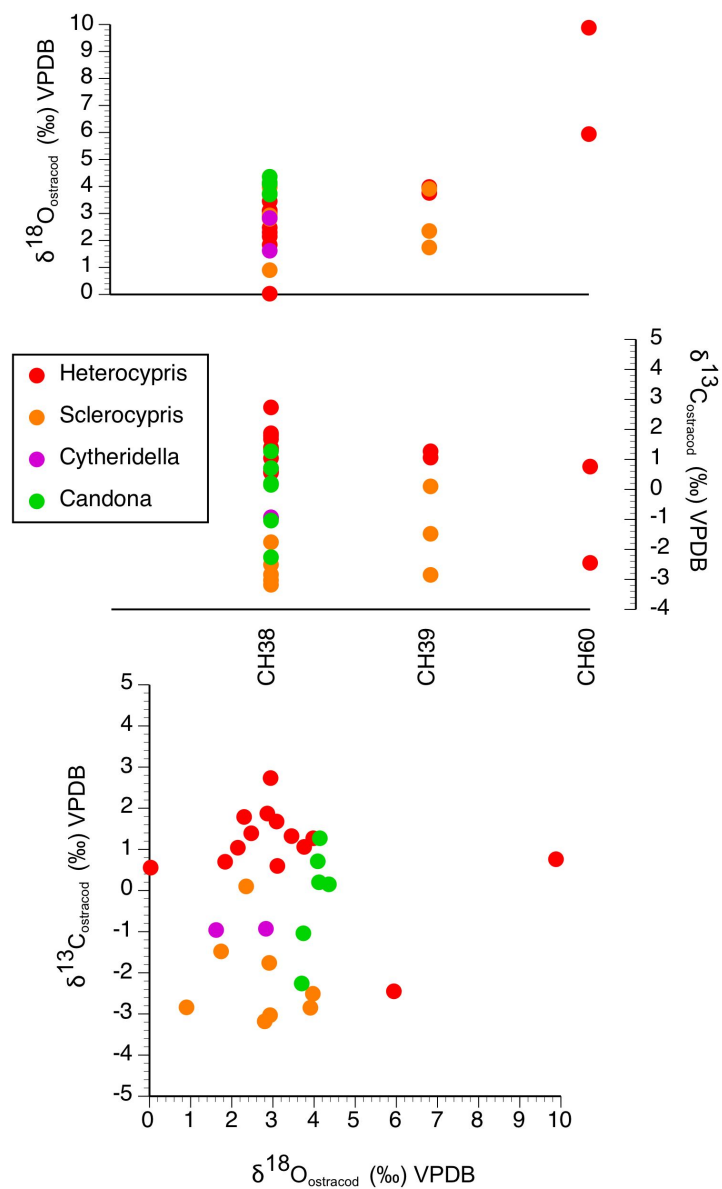
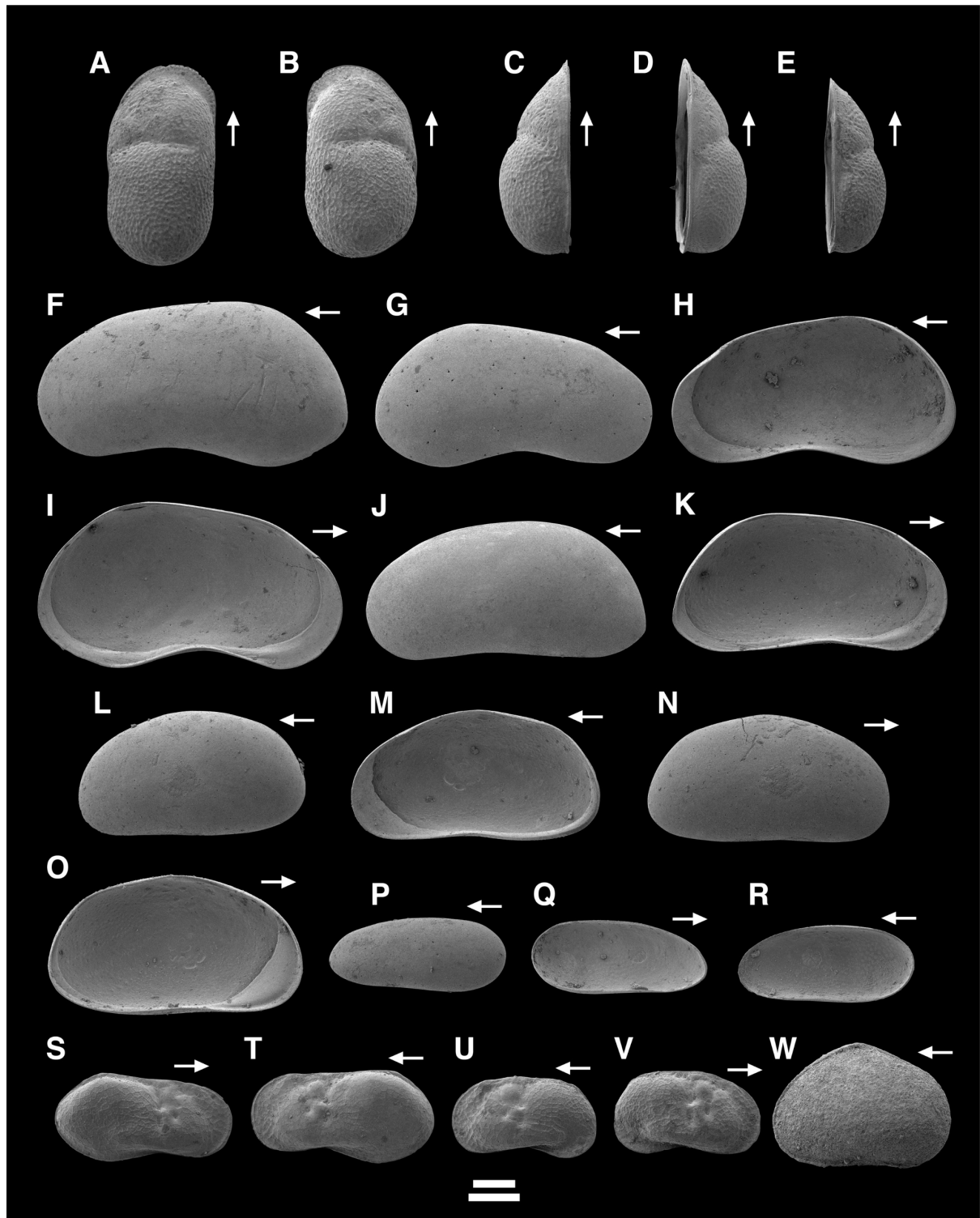


Fig. 7. Oxygen and carbon isotopes in ostracods and oxygen v carbon isotope cross plot

1170



1171

1172

1173

1174

- 1175 Fig. 8. SEM images of ostracods. All specimen from sample CH38. Scale bars:  
1176 200µm. Upper, A-O; lower P-W. Arrows point in anterior direction.
- 1177 (A) *Cytheridella tepida*. External lateral view of female right valve.  
1178 (B) *Cytheridella tepida*. External lateral view of female left valve.  
1179 (C) *Cytheridella tepida*. Dorsal view of female left valve.  
1180 (D) *Cytheridella tepida*. Dorsal view of female right valve.  
1181 (E) *Cytheridella tepida*. Dorsal view of A-1, right valve.  
1182 (F) *Candona cf neglecta*. External lateral view of left valve.  
1183 (G) *Candona cf neglecta*. External lateral view of right valve.  
1184 (H) *Candona cf neglecta*. Internal lateral view of right valve.  
1185 (I) *Candona cf neglecta*. Internal lateral view of left valve.  
1186 (J) *Candona cf neglecta*. External lateral view of left valve.  
1187 (K) *Candona cf neglecta*. Internal lateral view of left valve.  
1188 (L) *Heterocypris giesbrechtii*. External lateral view of left valve.  
1189 (M) *Heterocypris giesbrechtii*. Internal lateral view of right valve.  
1190 (N) *Heterocypris giesbrechtii*. External lateral view of right valve.  
1191 (O) *Heterocypris giesbrechtii*. External lateral view of left valve.  
1192 (P) *Darwinula stevensoni*. External lateral view of left valve.  
1193 (Q) *Darwinula stevensoni*. Internal lateral view of left valve.  
1194 (R) *Darwinula stevensoni*. External lateral view of left valve.  
1195 (S) *Limnocythete inopinata*. External lateral view of male right valve.  
1196 (T) *Limnocythete inopinata*. External lateral view of male left valve.  
1197 (U) *Limnocythete inopinata*. External lateral view of female left valve.  
1198 (V) *Limnocythete inopinata*. External lateral view of female right valve  
1199 (W) *Sarscypridopsis aculeata*. External lateral view of carapace from left side.

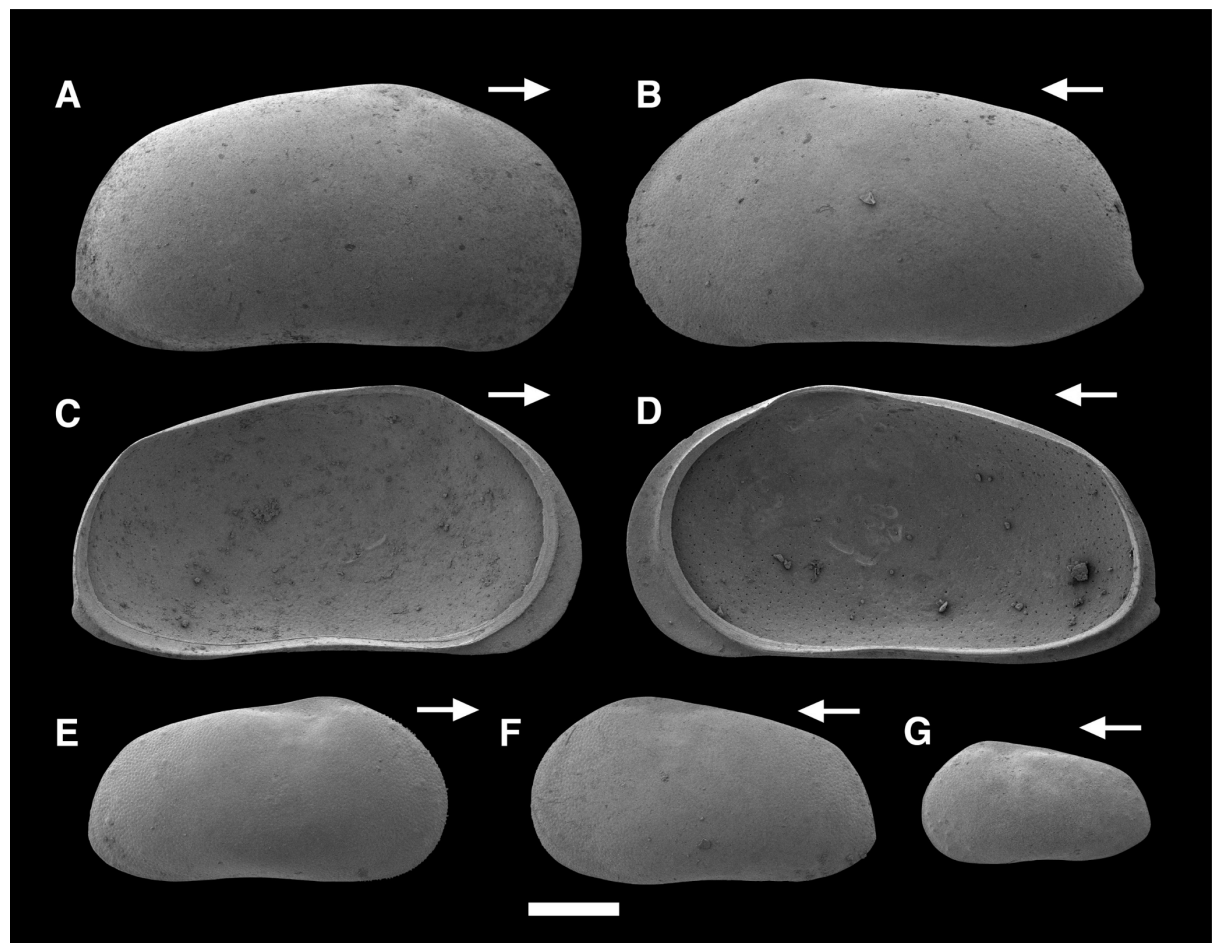


Fig. 9. SEM images of ostracods (continued) All specimen from sample CH38 Scale bar: 500µm. Arrows point in anterior direction.

(A) *Sclerocypris* cf *bicornis*. External lateral view of right valve

(B) *Sclerocypris* cf *bicornis*. External lateral view of left valve

(C) *Sclerocypris* cf *bicornis*. Internal lateral view of right valve

(D) *Sclerocypris* cf *bicornis*. Internal lateral view of left valve

(E) *Sclerocypris* cf *bicornis*. Internal lateral view of A-1, right valve

(F) *Sclerocypris* cf *bicornis*. Internal lateral view of A-1, left valve

(G) *Sclerocypris* cf *bicornis*. Internal lateral view of A-2, left valve



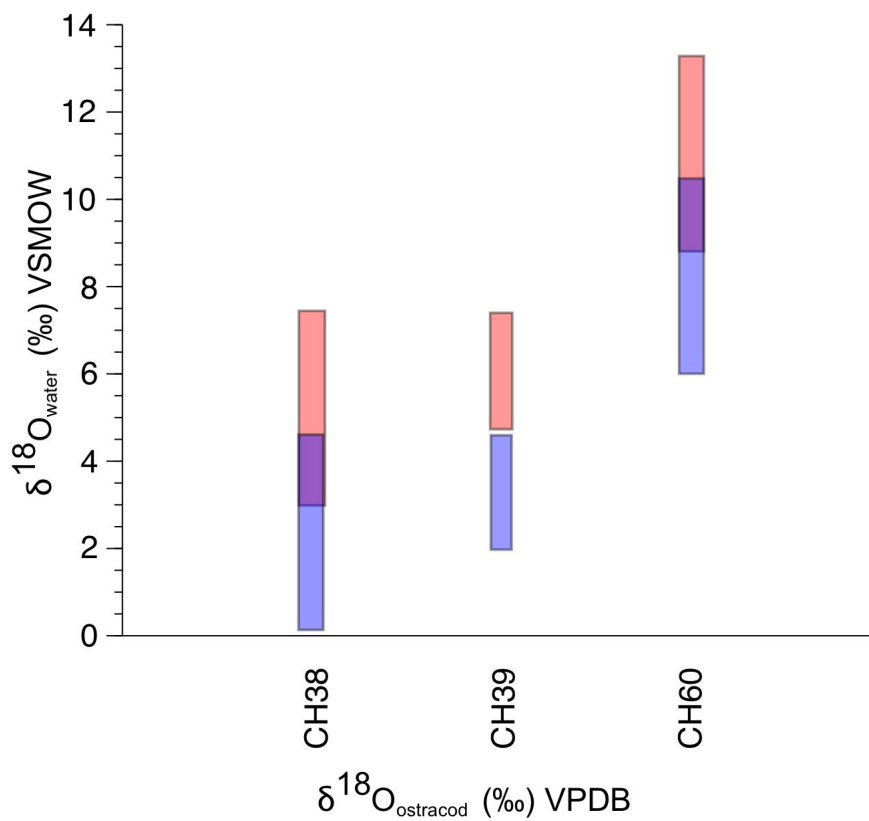


Fig. 10.  $\delta^{18}\text{O}_{\text{lake water}}$  values inferred from  $\delta^{18}\text{O}_{\text{ostracod}}$  at 21.2 ° (blue shading) and 31.4 °C (red shading) water temperature.

1227 **Tables**

1228 Table 1. New radiocarbon dates from the Angamma Delta section (CH37-CH39) and  
 1229 published date (Armitage et al., 2015) from the Bodélé Depression (CH60)

1230

Sample code	Laboratory reference	Material	Radiocarbon age ( $^{14}\text{C}$ BP)	Calendar age range ( $2\sigma$ ) (BP)	$\delta^{13}\text{C}$ ‰ VPDB
CH37	Beta-480211	Charcoal	6370 $\pm$ 30	7253 - 7416	-28.3
CH38-ostracod	Beta-480212	Ostracod shells - <i>Sclerocypris</i> cf. <i>bicornis</i>	4050 $\pm$ 30	4425 - 4784	-2.0
CH38-gastropod	SUERC-17169	Gastropod shells	4204 $\pm$ 37	4618 - 4849	-4.5
CH39	SUERC-20101	Ostracod shells - <i>Sclerocypris</i> cf. <i>bicornis</i>	3962 $\pm$ 37	4296 - 4522	-2.6
CH60	SUERC-18366	Bivalve shells - <i>Coelatura aegyptiaca</i>	1061 $\pm$ 37	926 - 1055	+0.3

1231

1232

1233 Table 2. Ostracod occurrences in Angamma Delta samples (numbers of valves  
 1234 counted)

	CH38	CH39	CH60
Dry weight of sediment (g)	30.8	9.4	6.9
<i>Limnocythere inopinata</i>	15	0	11
<i>Cytheridella tepida</i>	42	10	0
<i>Darwinula stevensoni</i>	13	0	1
<i>Candona</i> cf. <i>neglecta</i>	20	0	0
<i>Heterocypris giesbrechtii</i>	231	6	3
<i>Sclerocypris</i> cf. <i>bicornis</i>	54	6	0
<i>Sarscypridopsis aculeata</i>	1	0	0
Total	376	22	15

1235

1236

Table 3. Mollusc occurrences in Angamma Delta samples. For occurrences, √ denotes presence, no symbol denotes absence. For ecological preferences, √ indicates that the species is associated with that environment or condition, no symbol denotes no information and x indicates that the species is absent from that environment or is not known to tolerate the condition. Ecological data from Brown (1994), Van Damme (1984) and Ibrahim et al. (1999).

	CH38	CH59	CH60	River	Lake	Pond	Elevated salinity	Dessication
Gastropoda								
<i>Biomphalaria pfeifferi</i>	√	√		√	√	√		x
<i>Bulinus</i> cf. <i>jousseaumei</i>	√			√				x
<i>Corbicula consobrina</i>	√			√	√	√		
<i>Valvata nilotica</i>	√			√	√	√		
<i>Gabiella tchadensis</i>	√			√	√			
<i>Cleopatra bulimoides</i>	√			√	√	√		
? <i>Lymnaea natalensis</i>	√			√	√	√		(x)
<i>Melanoides tuberculata</i>	√	√		√	√	√	√	x
<i>Bellanya unicolor</i>	√			√	√	√		x
Bivalvia								
<i>Sphaerium hartmanni courteti</i>	√				√			
<i>Pisidium pirothi</i>	√			√	√	√	(√)	x
<i>Coelatura aegyptica</i>		√	√	√	√	√		

1267

[illegible]